LA--710

[redacted]

Series B

LA-710

Series B

[redacted]

28 October 1948

This document contains 80 pages.

NEUTRON FISSION CROSS SECTION OF U^{238} IN THE REGION OF NEUTRON ENERGY BETWEEN 6 AND 9 MEV

Work done by:

B. R. Curtis
K. W. Erickson
J. L. Fowler
L. Rosen
J. Slye
P. H. Snowden
R. Squires
E. Stovall, Jr.
F. K. Tallmadge

Report written by:

B. R. Curtis
J. L. Fowler
L. Rosen

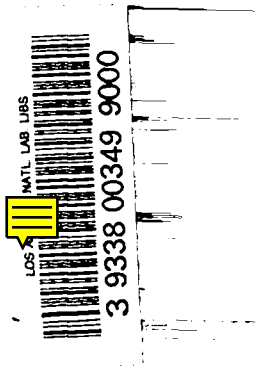

Abstract

Apparatus has been developed for using the cyclotron to produce effectively monoenergetic neutrons. The $D(d,n)He^3$ reaction is used, the bombarding deuterons being accelerated to about 10 Mev by the Los Alamos Cyclotron. The energy of these deuterons is determined by deflection in a magnetic field. The He^3 particles emitted into known solid angle and having known energy are counted by a proportional counter. A fission counter having foils on which is deposited uniform determined weights of U^{238} is placed in the path of the neutrons associated with the He^3 particles. Coincidences between the He^3 counter and the fission counter are recorded. The resolving time of the apparatus, and hence the accidental coincidences, are determined by moving the fission counter to such an angle that no real coincidences can occur. Since the proportional counter records the He^3 flux, and hence the associated neutron flux, the cross section of "28" is determined from the real coincidences per He^3 count and the thickness of the U^{238} in the path of the neutrons. The values of the cross section obtained together with the standard errors are:

$$\sigma\ (E_n = 8.8 \pm 0.5) = 1.17 \pm .11 \text{ barns}$$

$$\sigma\ (E_n = 5.6 \pm 0.5) = 0.68 \pm .14 \text{ barns}$$

$$\sigma\ (E_n = 8.9 \pm 0.5) = 1.04 \pm .12 \text{ barns}$$

NEUTRON FISSION CROSS SECTION OF U^{238} IN THE REGION OF NEUTRON ENERGY BETWEEN 6 AND 9 MEV

Introduction

At Los Alamos it is necessary to know the neutron fission cross section of U^{238} from the threshold to the region of 14 Mev (LA-610).

A number of investigators have determined the cross section for neutron energies below 3 Mev (see LA-520). With the $D(d,n)He^3$ reaction on the "long" electrostatic generator, the data has been extended to 5.85 Mev (LA-520). More recently, neutrons from the $T(d,n)He^4$ reaction have been used to obtain the cross section at 14 Mev and above (LAMS-777). There was, however, no standard way to produce monoenergetic neutrons in the region from 6 Mev to 14 Mev. In spite of the high neutron background associated with cyclotrons, a method has been developed to use the 10 Mev deuterons to produce effectively monoenergetic neutrons of energies between 6 and 9 Mev. The $D(d,n)He^3$ reaction is used where only fissions in coincidence with He^3 particles are counted. (The cross section for this reaction at 10 Mev is sufficient for this problem). (LAMS-600, Phys. Rev. 73 648, (E-8)(648)).

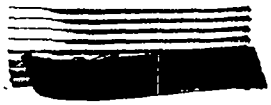

I. APPARATUS ASSEMBLY

In order to avoid the background in the immediate vicinity of the cyclotron, the deuteron beam was used 15 ft. from the cyclotron beyond the water wall shields. Fig. 1 shows the layout of apparatus. The deflected beam from the cyclotron is brought through 6" brass tubing to a wedge-shaped focusing magnet. From here the beam, being diaphragmed to $\pm$ 0.63°, passes through a gas target in the center of a 2 ft. diameter reaction chamber. Deuterium gas is contained in the target by mica windows over the entrance and exit ports and over a side tube for He^3 particles. These particles emitted into known solid angle, and hence having known energies, are counted by the proportional counter. The fission counter is rotated in a horizontal plane until it is centered on the cone of neutrons associated with the He^3 particles. The deuteron beam is monitored by a Faraday cup and recorded by an electronic current integrator.

From time to time the energy of the beam is determined by lifting the Faraday cup out of the path of the beam and allowing the beam to pass through slits and then between the poles of the analyzing magnet. A simultaneous measurement of the deflection of the beam and the magnetic field gives the deuteron energy.

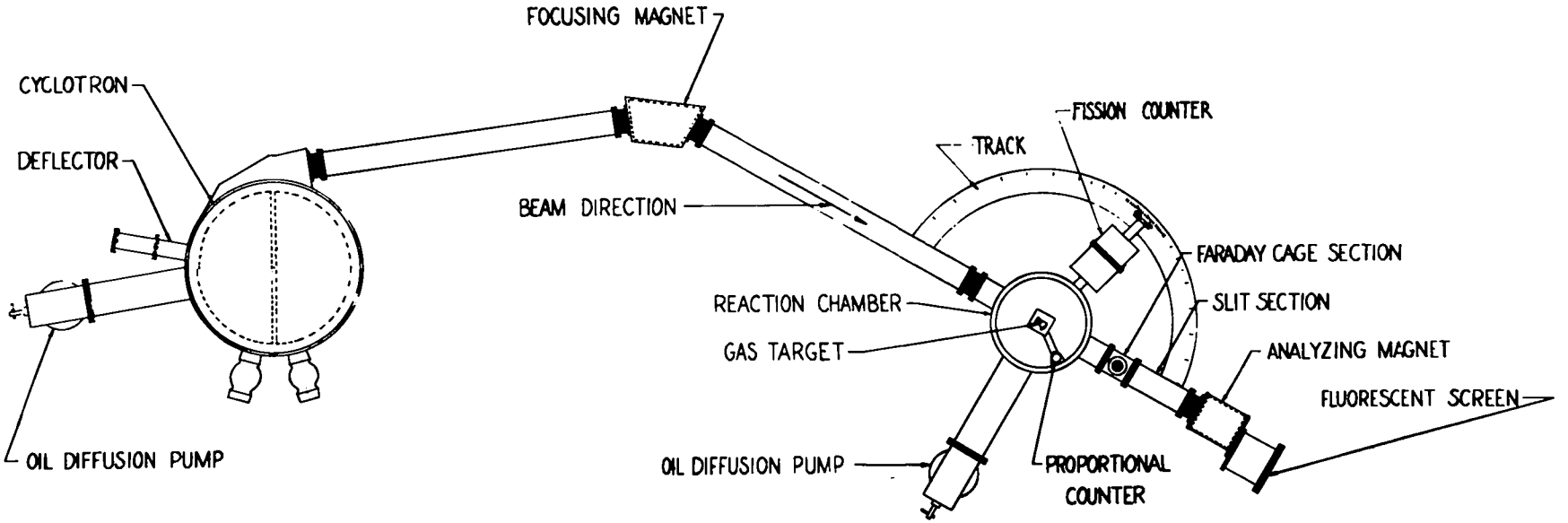

VACUUM SYSTEM

[redacted]

FIG 1

APPROVED FOR PUBLIC RELEASE

During a run the number of He^3 particles, the number of fissions, and the number of coincidences between them are recorded electronically. The number of accidental coincidences is found from the resolving time of the apparatus (approximately 2 μs) which is determined experimentally by runs in which the fission counter is rotated at such an angle that there can be no real coincidences.

Figs. 2 and 3 are photographs of the scattering chamber, fission counter, and analyzing magnet.

Figs. 4 and 5 are top and side view assembly drawings of the reaction chamber, proportional counter, and fission counter. The reaction chamber proper, pump out leads, and side ports are of welded steel construction. The lid of the reaction chamber is a 1-1/2" thick safety plate glass which rests on two 1/4" x 1/4" thick rubber gaskets which are countersunk in grooves in the ring around the edge of the chamber. The bottom of this chamber is a 3/4" brass plate which contains a 1/4" gasket groove to make the vacuum seal to the chamber. In the center of the bottom plate is a 2" diameter Wilson seal through which the proportional counter can be rotated at the desired angle to the beam in the horizontal plane. The lead to the proportional counter passes through the center of its supporting arm. The proportional

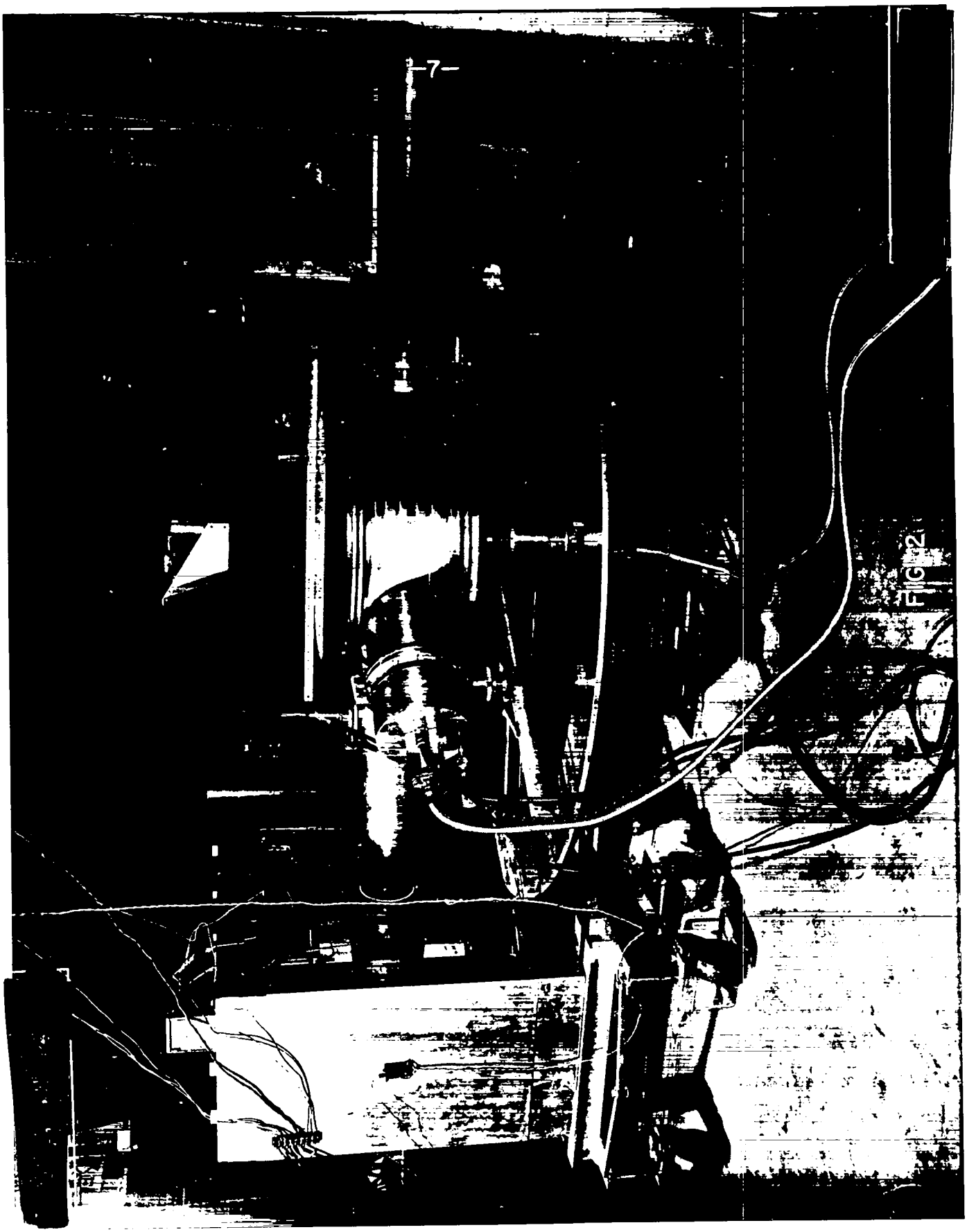

FIG. 2

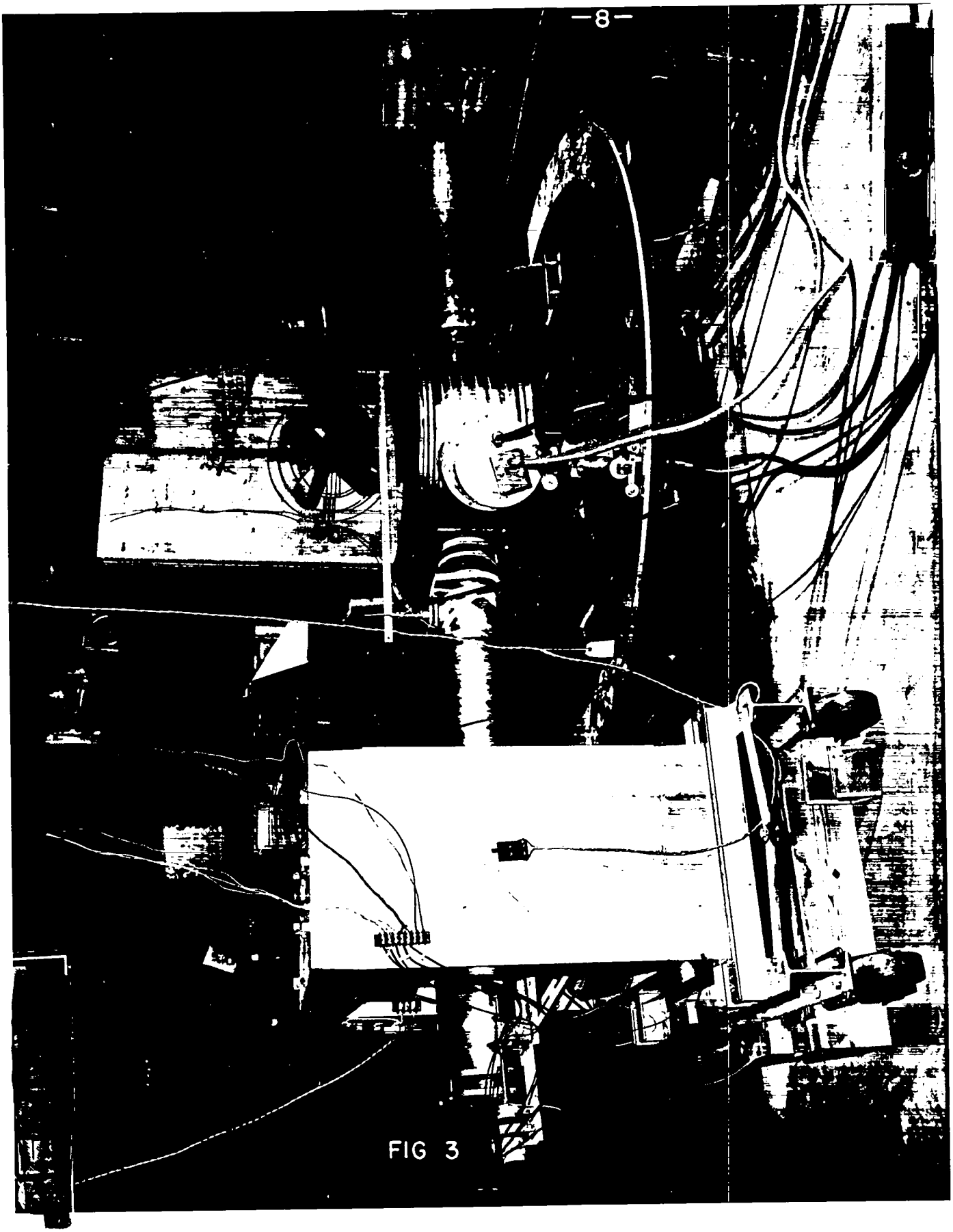

FIG 3

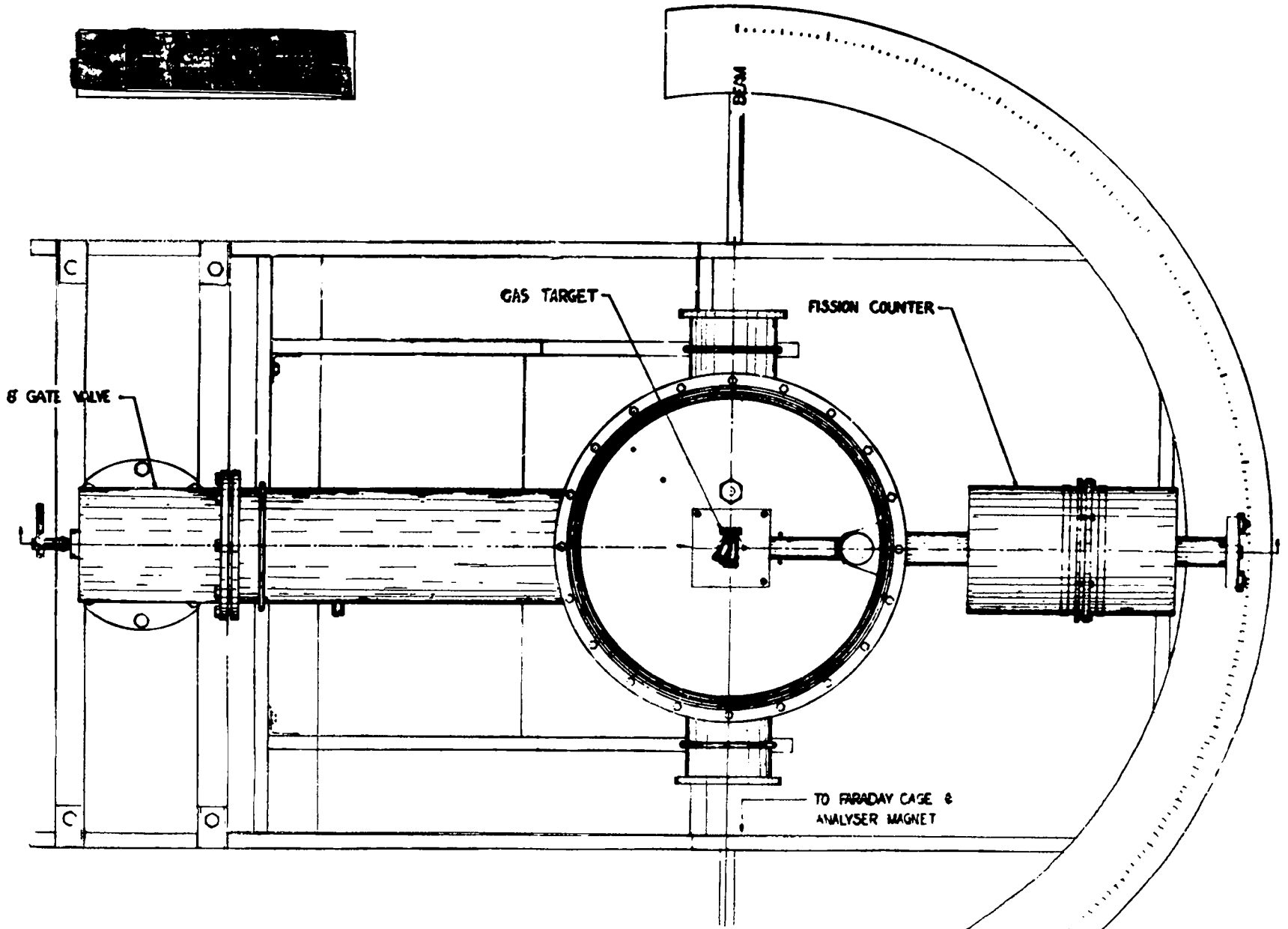

D-D REACTION CHAMBER

FIG 4

APPROVED FOR PUBLIC RELEASE

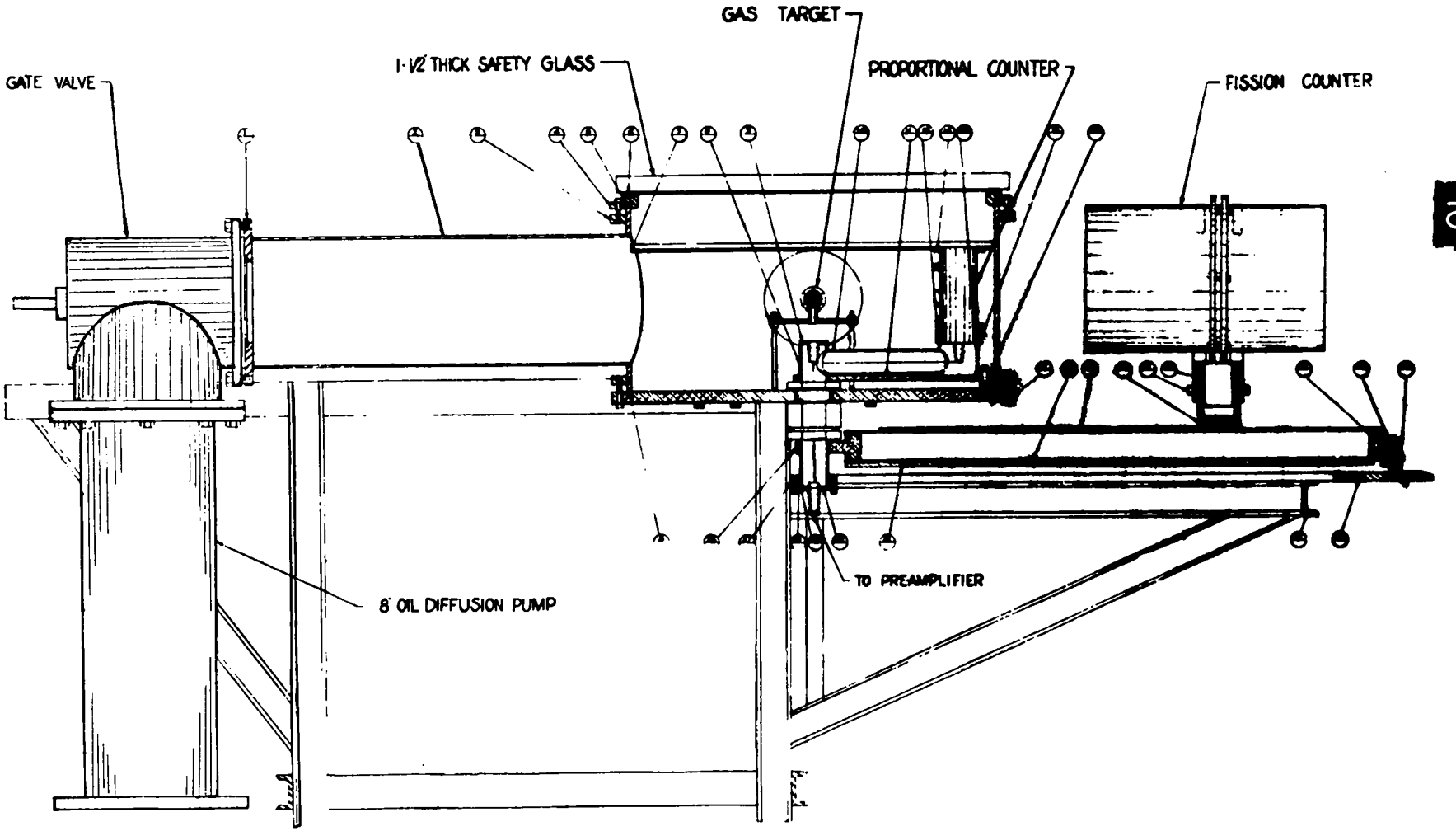

D-D REACTION CHAMBER

[redacted]

FIG 5

APPROVED FOR PUBLIC RELEASE

counter is so mounted that it can be adjusted in height relative to the base plate. The high voltage connections and preamplifiers which can be seen in the photograph of Fig. 2 are supported at the end of the 2" tube which passes through the Wilson seal. Mounted within the reaction chamber at about the top of the proportional counter is a ring accurately graduated in degrees from 0 - 360°. All angular measurements are referred to this ring. As can be seen in the drawing of Fig. 4, the fission counter is mounted on an arm outside of the reaction chamber and can be rotated at any angle from 0 - 180° about the center. The angular position of this counter can be read on graduations on a semi-circular track seen in Fig. 5, which is calibrated against the ring within the reaction chamber. The height and radial position of the fission counter are adjustable.

Fig. 21 is a drawing of a typical gas target, which is supported on a mount above the base plate such that it can be lined up with the geometrical center of the reaction chamber. The windows over the ports are mica of thickness from 1-3 mg/cm^2 depending on the angular region being investigated. The target is so constructed that the proportional counter can only see the beam where it is bombarding the target gas, and hence the charged particle background due to bombardment

of windows, etc., is eliminated. Similar targets were used in which the side ports make angles of 20° and 30° with the beam axis.

Fig. 6 is a drawing of the Faraday cage section, showing how the Faraday cage can be removed from the path of the beam by means of the Wilson seal. Permanent bar magnets arranged to give a field at the bottom of the cup perpendicular to the axis of the beam immobilize secondary electrons produced by the beam.

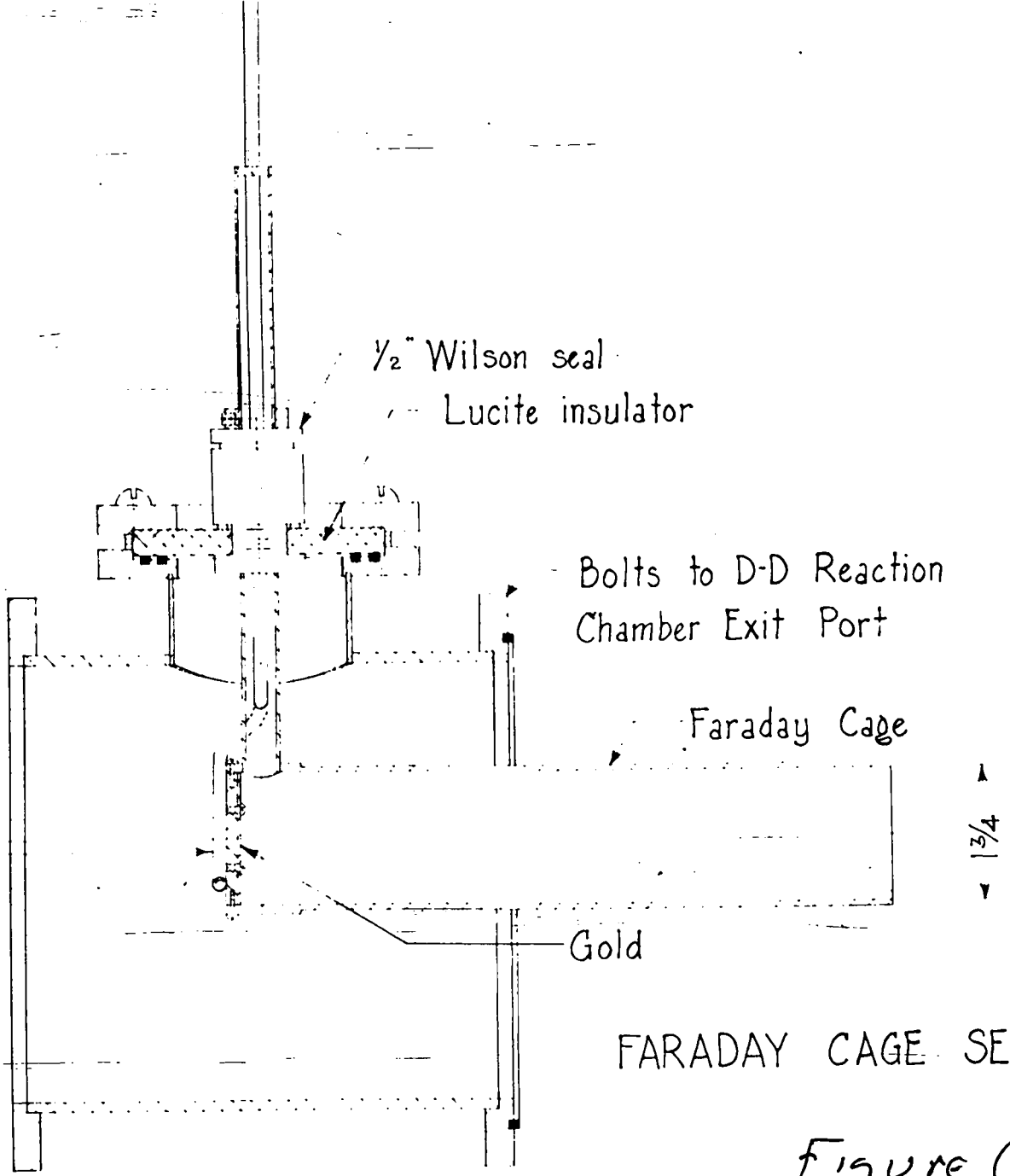

FARADAY CAGE SECTION

Figure 6

APPROVED FOR PUBLIC RELEASE

II. FOCUSING THE CYCLOTRON BEAM

In many experiments associated with a cyclotron it is desirable to have the beam some distance from the accelerating chamber, both for the reduction of neutron background and for the ease of installation of experimental apparatus. This was accomplished during the war by Feynman, Lavatelli, and Sutton (LAMS-514) who used a wedge-shaped magnet to focus a fairly intense beam of deuterons outside of the cyclotron water shield about fifteen feet from the cyclotron.

The general method outlined in the above report was followed. Considerable time was spent adjusting the position of the focus magnet and the target chamber so that the best possible focus was obtained. These adjustments were greatly facilitated by the use of a television pickup and camera which permitted continuous observation of the focused spot of deuterons, as observed on a willemite (zinc orthosilicate) screen placed at the end of the exit tube. By this means the best focal distance was determined and also the best position of the focus magnet with reference to the target. The outline of the essential apparatus is shown in Fig. 7. The willemite screen was placed on a glass plate at the end of a telescoping tube which could then be adjusted to any desired distance and the effect on the focus

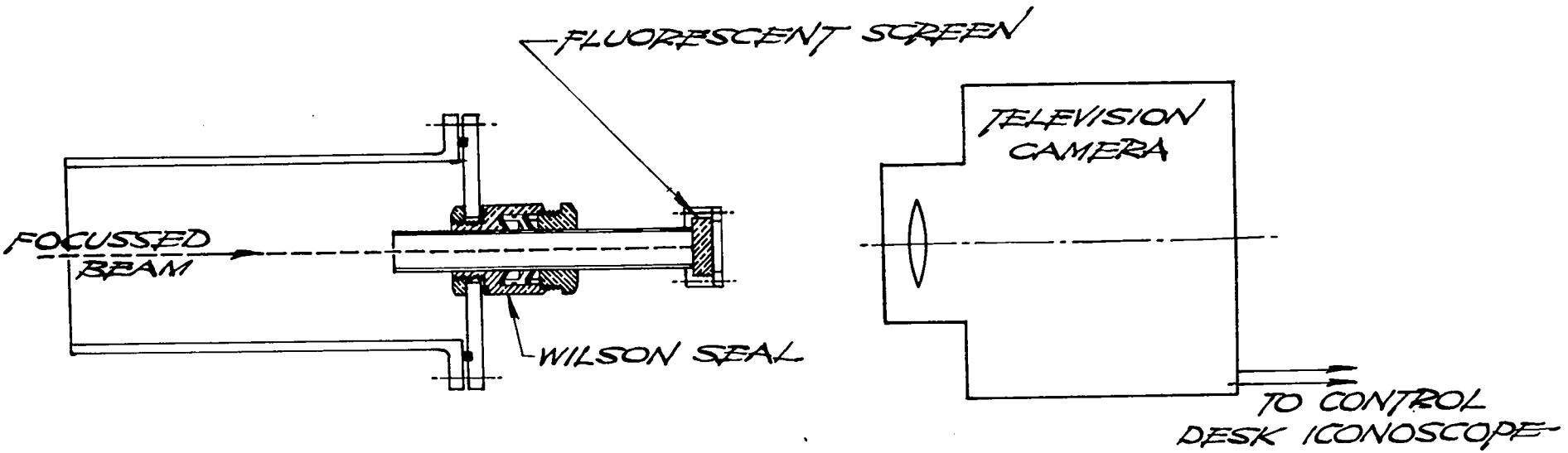

FIG. 7

EQUIPMENT FOR ADJUSTING FOCUS CONDITIONS

APPROVED FOR PUBLIC RELEASE

observed. The focused spot was approximately 1/4-inch wide by 3/4-inch high and under the optimum operating condition a beam of 5 microamperes of 10 Mev deuterons could be obtained over this area.

One additional piece of equipment was added, namely an electronic control (designed by H. T. Gittings - LAMS-678) for the focusing magnet field so that it could be maintained constant throughout any given experiment.

Since the gas target is located approximately at the focus point of the wedge-shaped magnet (300 cm from the focusing wedge) the beam converges as it enters the target and diverges as it leaves the center of the scattering chamber. In order to restrain the beam to a known direction a slit 1-1/8" wide by 13/16" high was placed between the focus magnet and the scattering chamber at a distance of 71.6" from the target and a gold diaphragm with a 1/2" hole placed at the target entry port so that the beam was defined to $\pm$ 0.63 degrees in the horizontal and $\pm$ 0.53 degrees in the vertical direction.

To determine the exact direction of the beam as it passes through the gas target chamber, a small aperture (1/8" diameter) Faraday cup was mounted on the proportional counter. This was moved through the beam and the current picked up by the cup measured by a

DC amplifier. Thus the angular spread of the beam could be measured and its angular direction in passing through the scattering chamber determined. A sample curve of the angular spread is shown in Fig. 8. This is the spread expected from the geometry of the experiment. Rutherford scattering due to the front window of the gas target does not increase appreciably the angular spread, since only about 0.4% of the beam would be scattered more than one degree.

Under normal operating conditi ns one obtains a beam of deuterons on the exit port from the cyclotron which is sensitive to deflector voltage. With a high deflecting voltage the beam hitting the outside of the focus magnet may be 25 microamperes; by lowering the deflector voltage a beam of approximately 10 microamperes hits the inside of the exit tube. For optimum conditions one adjusts for the valley between the two peaks, which indicates that the maximum is hitting the 5" x 1/2" opening through the focus magnet. Conditions can also be varied so that very little current is striking the exit tube, which is desirable for the reduction of background.

The position of the deflector tilt is quite important to obtain a maximum beam at the target. In general, a tilt toward the Dee reduces the deflector

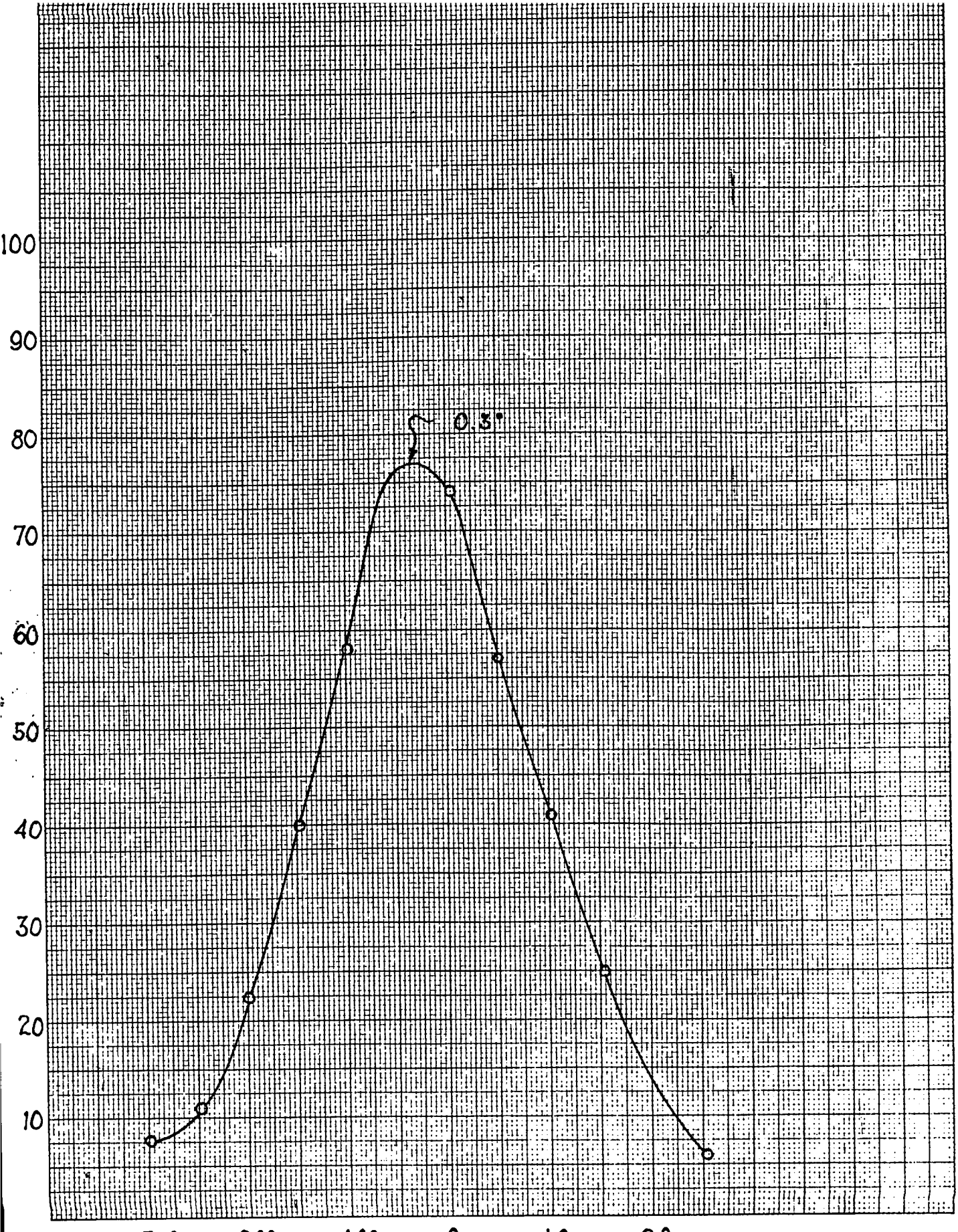

voltage necessary to hit the focus magnet; a tilt away increases the voltage required.

The beam current was measured by means of a Faraday cage (Fig. 1) connected to an electronic current integrator (DWG. #704). The cage could be lifted through a Wilson seal, so that the beam could pass through the slit section and into the analyzing magnet, when the energy of the beam was measured.

III. ENERGY MEASUREMENT

The energy of the beam of deuteron ions was measured by a magnetic deflection method following the general procedure described by Creutz and Wilson (RSI 17, 385, 1946). This involves the measurement of the deflection of the deuteron beam and the simultaneous measurement of the magnetic field causing the deflection.

A. Experimental Arrangement:

The experimental arrangement is shown in Fig. 9. It consists of a magnet with rectangular pole pieces (28.54 x 25 cm), a fluorescent screen for observation of the deuterons, and a single turn rectangular flux coil for measurement of the field. An adjustable slit section is provided between the gas target and the analyzing magnet to define the beam.

The energy of the deuteron beam is given approximately by the following formula, which is derived from the equations of motion (see Appendix I):

$$W = \frac{e^2A^2}{2M_oc^2}\left(1 - \frac{W}{2M_oc^2}\right) \times \left[1 + \left\{\frac{a + b/2(1-e^2A^2/8M_oc^2W)}{D}\right\}^2\right] \quad (1)$$

where W is the energy of the deuteron beam in ergs, D is the deflection as measured on the fluorescent screen, e is the charge on the deuteron, M_o the rest mass of the deuteron, a and b are dimensions of the apparatus as shown in Fig. 9.

APPROVED FOR PUBLIC RELEASE

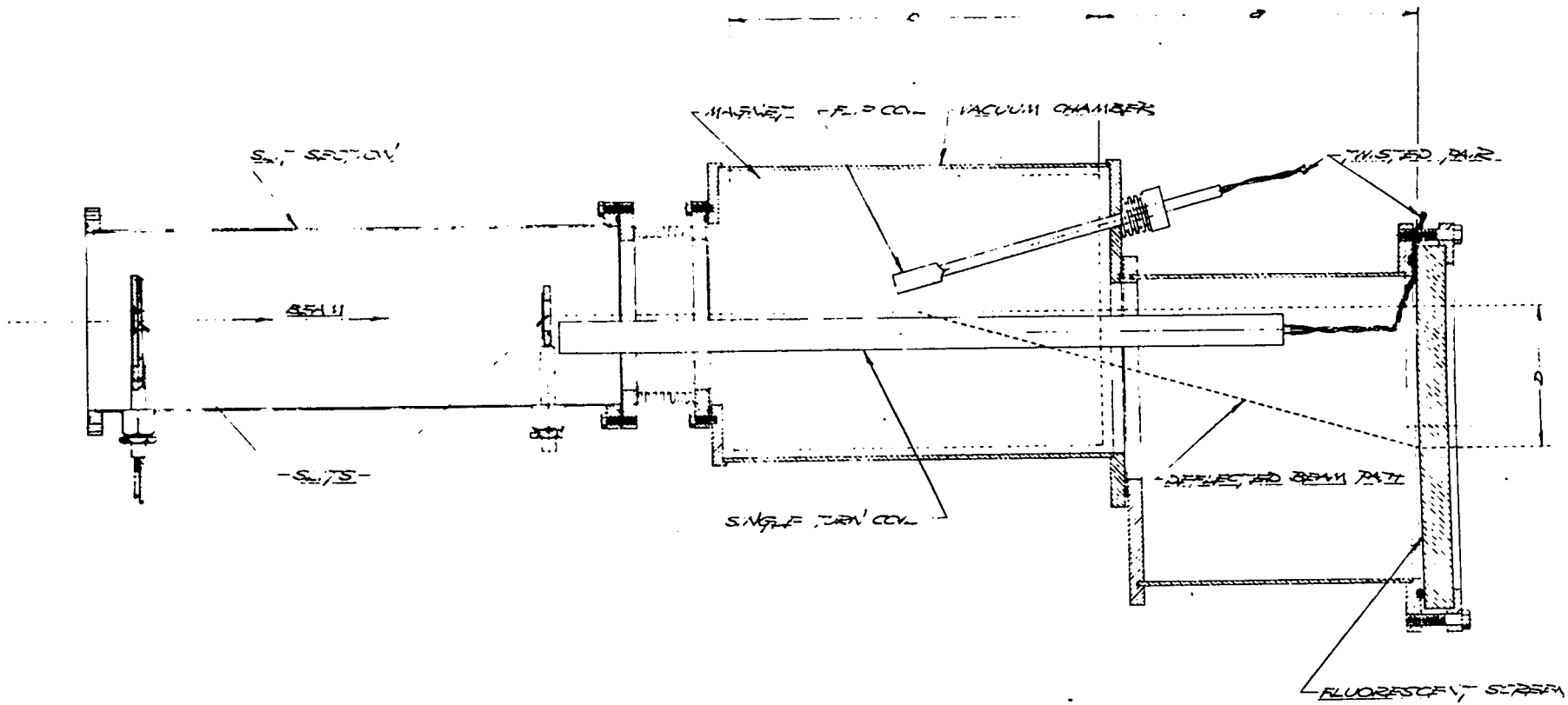

FIGURE 9

ENERGY MEASURING SECTION

B. Measurement of Field:

The quantity A in Equation (1) is equal to $\int Hdx$ where H is the change in magnetic field produced by breaking the magnetizing current and x is measured along the initial direction of the deuteron beam. The value of A is determined by use of the single turn coil of width W which extends through the magnetic field from a zero field region on one side of the magnet to a zero field region on the other. The ends of this coil are brought out with a twisted pair to reduce the effect of stray fields and connected to the secondary of a mutual inductance M as shown in Fig. 10. The coil was constructed by winding a single turn of 0.001 inch copper strap around a rectangular lucite form. The form was accurately machined so that the width, W, of the completed coil was 1.033 ± 0.002 inches. The total flux as measured with the coil is equal to $w \int Hdx$ which is equal to $M \Delta I$ where ΔI is the current through the primary of M necessary to balance out the emf developed by the change in flux through the coil. The current ΔI was measured with a potentiometer bridge and standard resistance.

Since in this method only a single deflection was measured rather than reversing the magnetic field, as was the case in the method of Creutz and Wilson,

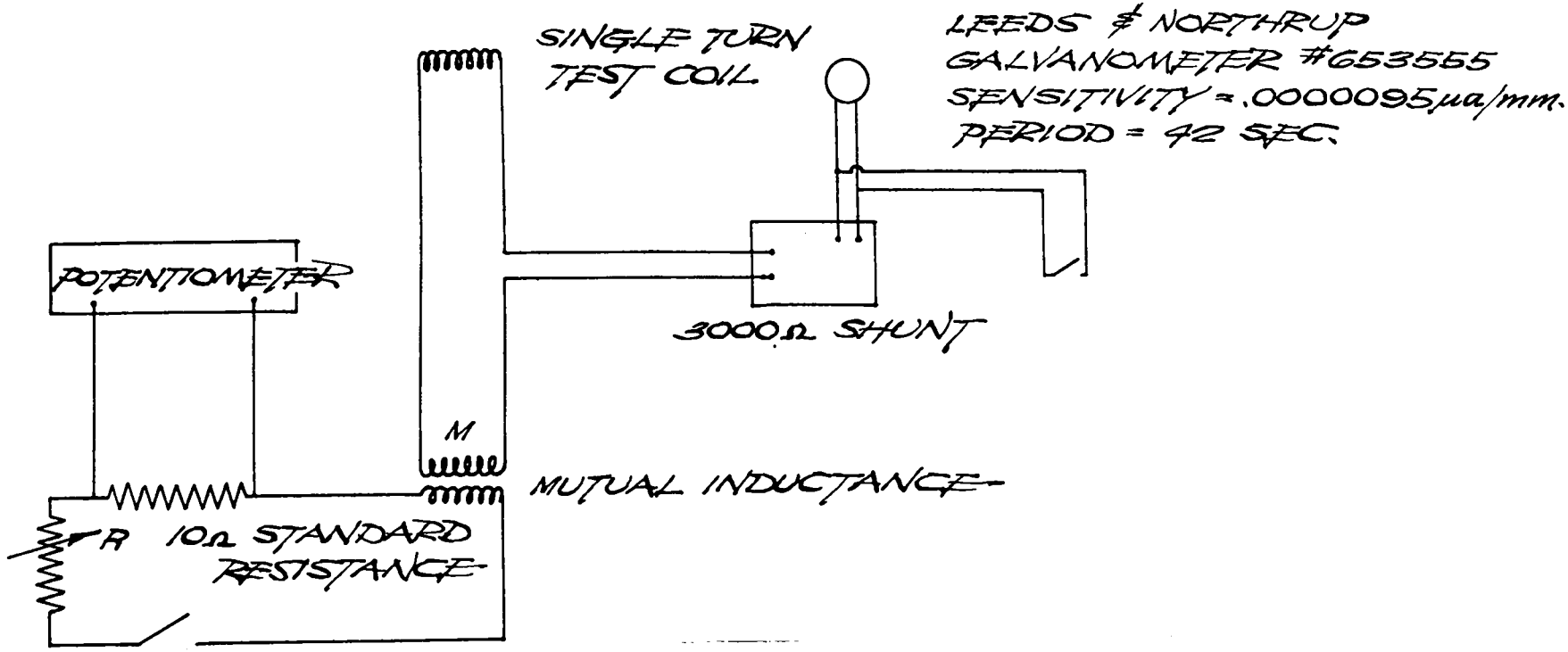

FIG. 10

CIRCUIT FOR MEASURING MAGNETIC FIELD

APPROVED FOR PUBLIC RELEASE

a small correction was necessary for the residual field of the magnet. This was obtained by using a small flip coil, which was calibrated against the single turn coil so that the residual field could be measured and the correction applied. Since the residual field causes compensating correction in both D and H the correction to the energy is small. The advantage of measuring the field by breaking the current to the magnet rather than reversing this current lies in the fact that the time constant in the former case is short enough to eliminate a correction for galvanometer drift.

C. Discussion of Errors:

The mutual inductance used in these experiments is calibrated by Leeds and Northrup to ± 0.5% accuracy. It was compared with two other inductances and found to agree within 0.2%.

The width of the undeflected deuteron beam was approximately one mm wide. When deflected the width increased about 0.5 mm, indicating a spread of energy within the beam of approximately 1%. The position of the beam could be read to 0.5 mm in 160 mm, or a maximum error of 0.3%.

The geometrical constants a, b, and w could be measured to better than 0.2%.

Since the energy is proportional to A^2/D^2

the expected accuracy is of the order of ± 2%.

Since a null method is used for measurement of the flux the error introduced by galvanometer drift is negligible.

Examples of energy measurements for three runs are given in Appendix II.

D. Absorption Measurements:

Several tests were made using aluminum absorbers to take out most of the energy of the deuteron beam and then varying the gas pressure in the target chamber to give a range-absorption curve for the beam. The results of the method showed essential agreement with the magnetic deflection method and indicated that no large error existed, i.e., a shorted pick up coil, etc..

IV. ELECTRONIC EQUIPMENT

Fig. 11 is a block diagram of the electronic equipment used. All of the equipment is of standard design and is identified by the following designations:

Pre-amplifiers and main amplifiers	- Model 500
Coincidence Circuit	- Dwg. 808
Current Integrator	- Dwg. 704
Scalers	- Model 200
Mechanical Counter	- Cyclotron Specialties Co.
10 Channel Amplitude Analyzer	- Model 301
Precision Pulser	- Model 100

The only change made in the electronic equipment consisted in replacing the R-C clippers in the main amplifiers with delay line clippers which reduced the pulses to about 1/5 of their original amplitudes in about 2 μs.

This was accomplished by terminating the last cathode follower in the pre-amplifier with a resistance to ground equivalent to the input resistance of the main amplifier, and inserting between the output of the pre-amplifier and the input of the main amplifier the circuit shown in Fig. 12.

Each channel of the coincidence circuit produced pulse gates 0.85 μs wide. The resolving time of the coincidence circuit was experimentally determined

BLOCK DIAGRAM OF ELECTRONIC EQUIPMENT

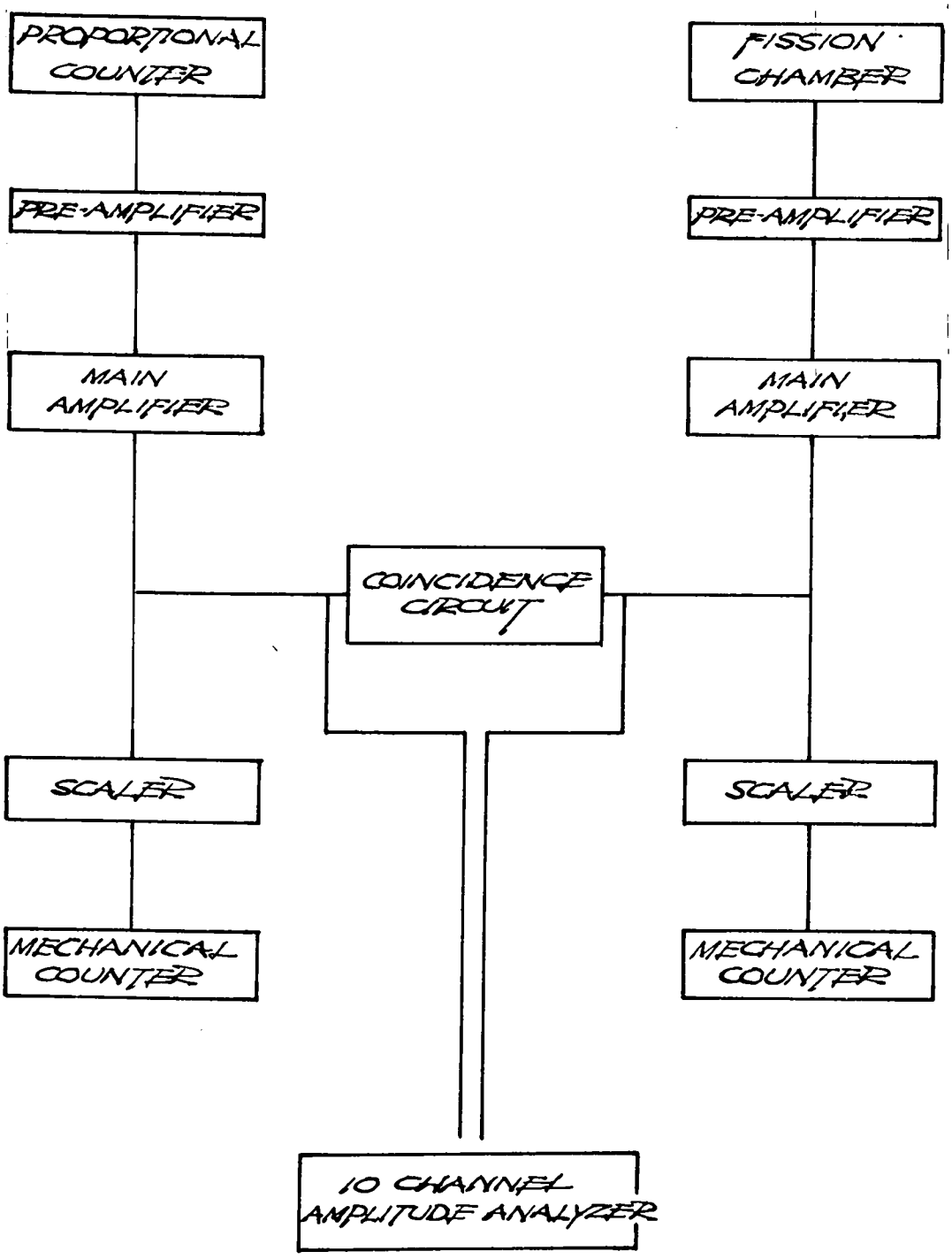

FIG. 11

DELAY LINE CLIPPER ARRANGEMENT USED WITH AMPLIFIERS

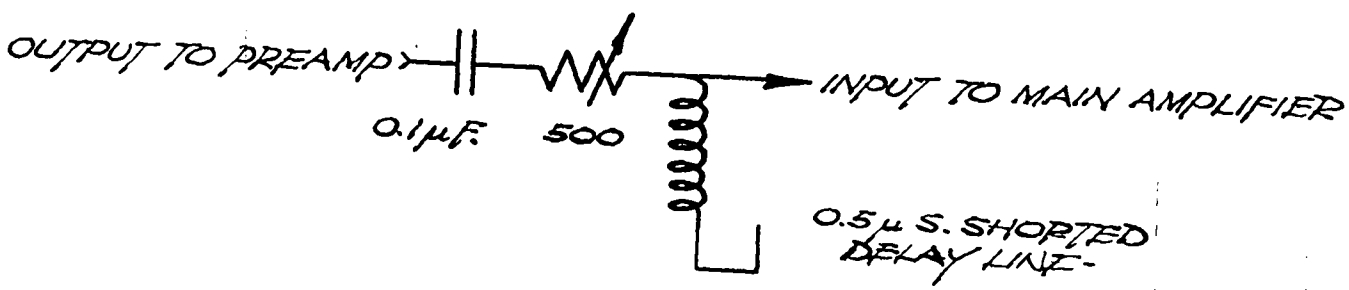

FIG. 12

with the same counters used in the actual experiment, as described in Section VIII. -·H. This experimental resolving time came very close to the previously determined electronic resolving time.

A precision pulser was used to intercalibrate amplifiers, discriminators, and 10 channel amplitude analyzer at the beginning and end of approximately each four-hour period.

V. FISSION COUNTER

Fig. 13 is a sectional assembly of the fission chamber used. It consisted of 13 plates, 7 of which served as collectors while the other 6 served as the high voltage electrodes and contained U^{238} foils on both sides. Each plate was made of 1/32" dural, the spacing between plates being 0.396". The counter was filled with argon to a pressure of 35#/sq. inch above atmosphere. This pressure was more than sufficient to stop the most energetic fission particles before they reached the collecting electrodes. The gas filling was renewed every 12 hours in order to avoid changes in pulse sizes due to accumulation of impurities in the gas. A voltage of 4000 volts, well filtered by a π network of resistors and capacitors, was applied to the high voltage electrodes. It was determined that changing the voltage by 1000 volts in either direction had no effect on the number of pulses recorded at the bias setting employed.

The fission pulses, as seen on an oscilloscope, had a rise time of slightly less than 1 μs and a width of about 2 μs. Random noise was considerably lower than the pulses produced by the α- particles from the active material. α pileup was negligible. The U^{238} foils for this experiment were made by R. W. Potter. The foils were made by the Zapon technique, the painting

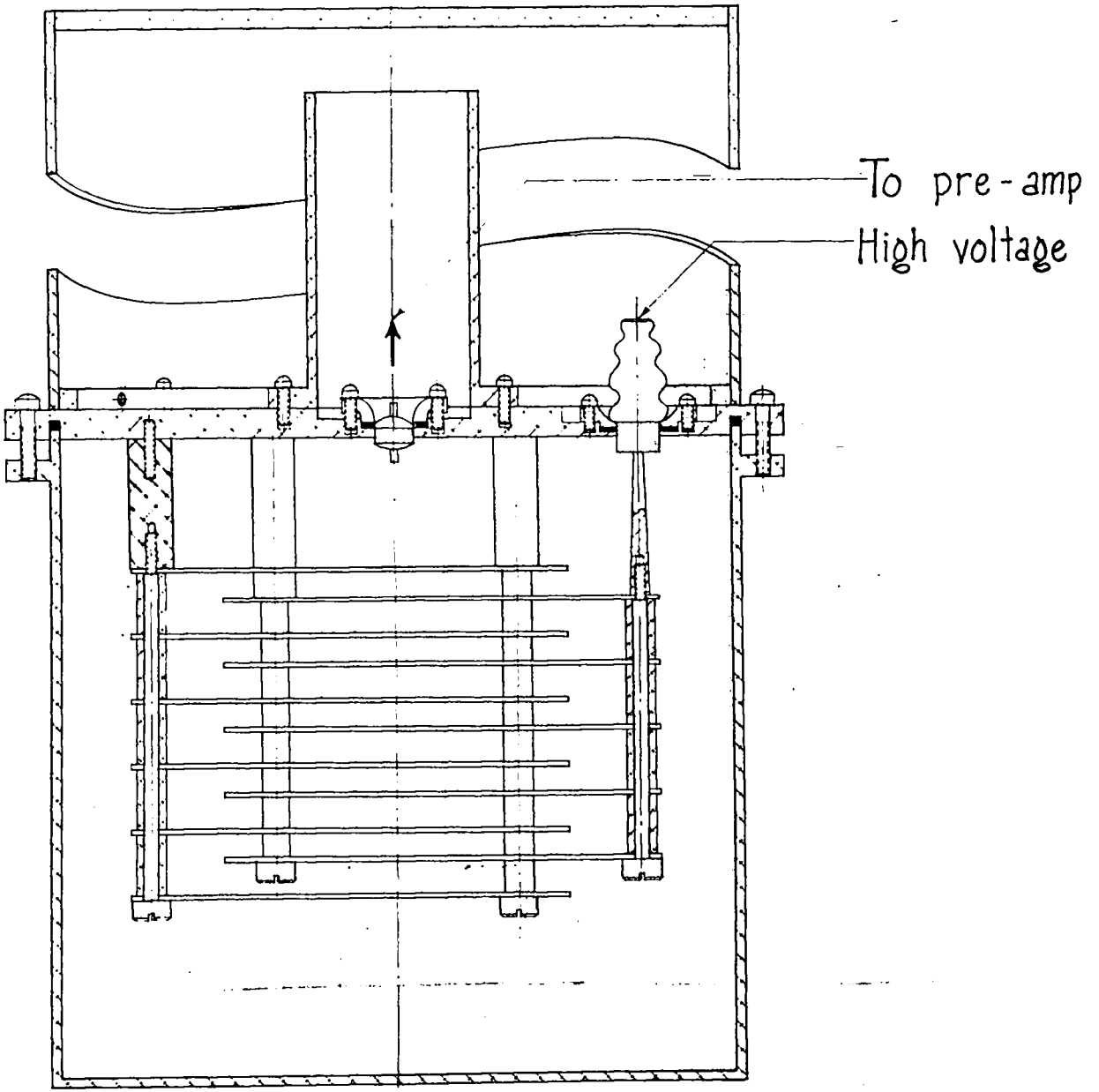

FIGURE 13
Fission Counter

APPROVED FOR PUBLIC RELEASE

being done mechanically on an endless belt moving past a stationary brush into which was fed the Zapon solution containing U^{238}. By this method it was possible to obtain foils which were uniform in thickness to better than 10%. The uniformity of the foils was determined by placing each foil in contact with an α-particle sensitive photographic emulsion for an appropriate time. After exposure the plates were processed and examined under a microscope and the number of α-particles/unit area was determined for 10 to 12 areas on each foil. This determined the uniformity of the foils over very small areas ($\sim$ 0.1 mm^2). Fig. 14 is a plot of the number of tracks per unit area as a function of distance from the center of a typical foil. Although the non-uniformities did exhibit somewhat of a pattern, most of this was eliminated by the ramdom mounting of the foils in the counter. The foils were mounted on the dural high voltage plates with liquid porcelain cement. This eliminated most of the impurity difficulties which are involved when one uses lucite or duco cement. Even so, it was found desirable to expose the plates to a fairly good vacuum ($\sim 10^{-4}$ mm Hg) for 24 hours after the foils were mounted. Fig. 15 gives the energy distribution of the fission fragments as observed in the fission counter under normal operating conditions.

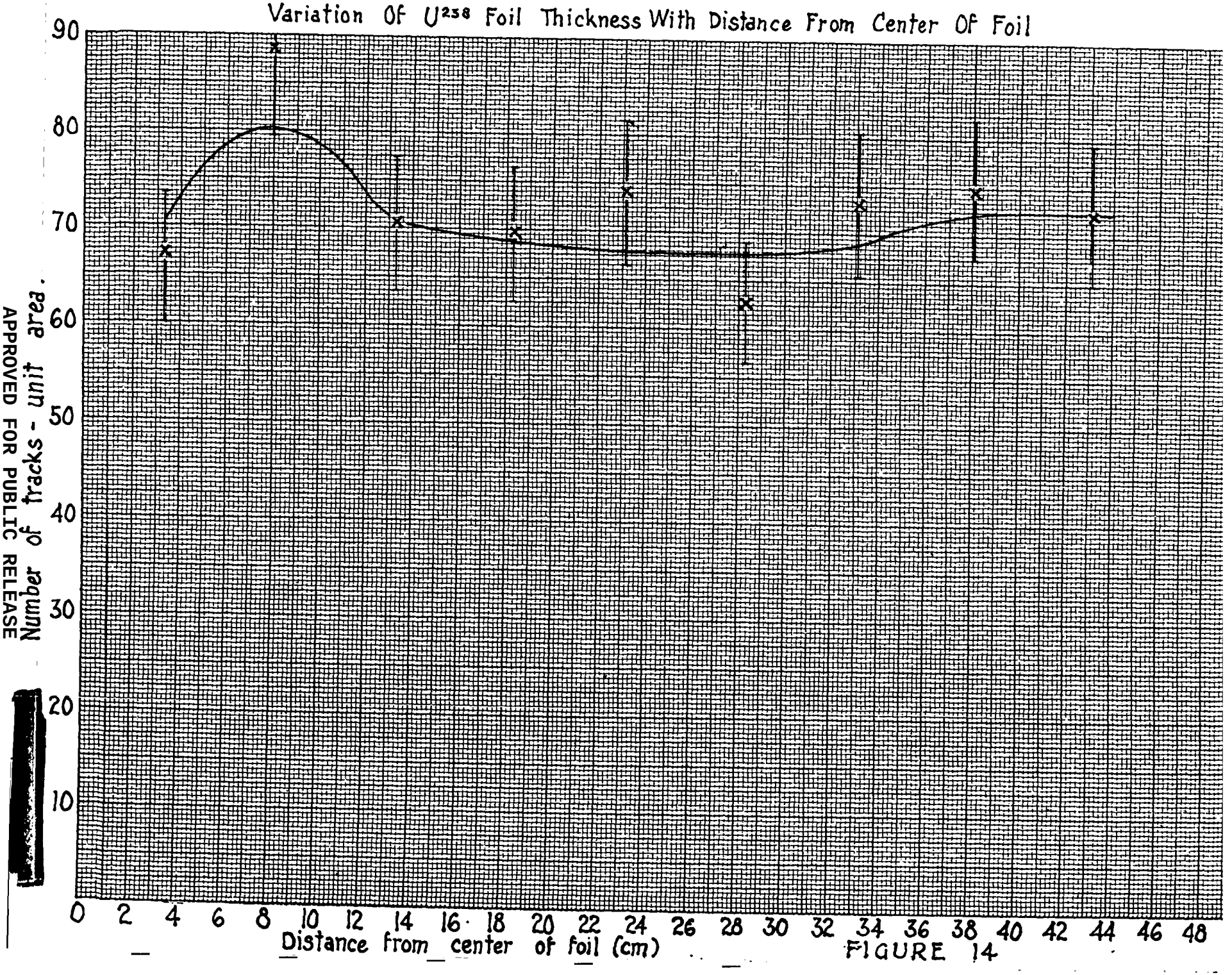

FIGURE 14

APPROVED FOR PUBLIC RELEASE

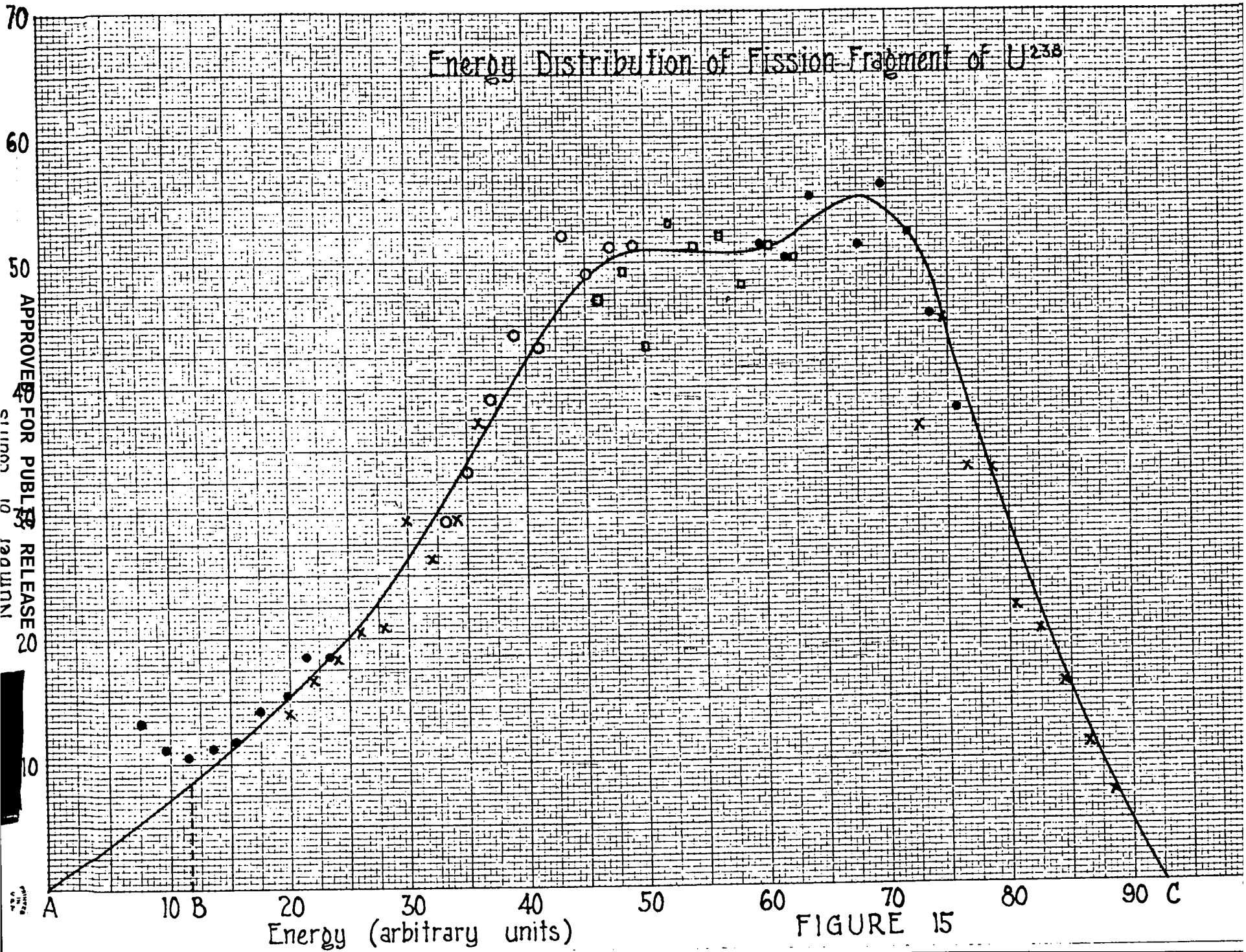

FIGURE 15

Even more important than an accurate determination of the uniformity of the U^{238} foils is the determination of the actual thickness of the U^{238} foils, since this enters directly into the equation for the cross section. The correction that must be made to the observed number of fissions can be divided into two parts: a correction for the fraction of fissions not observed because of complete absorption of the energy of the fragments of U_3O_8; and a correction for the fraction of the fissions not observed because the fragments which did penetrate the U_3O_8 did not have sufficient energy to overcome the bias setting. Now this latter correction is quite easy to make from Fig. 15. Since the bias setting was arbitrarily fixed at point B, the curve was integrated from A to B and from B to C. The number of observed fissions were then multiplied by $\frac{\int_A^B + \int_B^C}{\int_B^C}$ to give the number of fissions which occurred and yielded fragments which penetrated the foil. This correction amounted to only 2%. There still remains the determination of the absolute thickness of the foil and the total self-absorption, i.e., absorption which prevented fragments from penetrating the foil. It appeared that the simplest and most accurate procedure for making both determinations was to determine the "effective" thickness of the U^{238} for fission fragments,

i.e., F x total thickness where F is the fraction of all fission fragments which are completely absorbed in the U_3O_8. This was accomplished as follows: a determination was made of the energy distribution of the α-activity of each of the foils over an accurately determined area in a Frisch-grid ionization chamber, utilizing the 10 channel discriminator. Fig. 16 is a plot of such a determination. These curves were extrapolated to zero and integrated to yield the total activity of each of the foils. Since the specific activity of this U^{238} sample was known to $\pm$ 0.5% this immediately gave the effective thickness of the foils for particles of energy 4.75 Mev, i.e., the total thickness - F_1 x total thickness when F_1 = fraction of all alphas not counted because they were completely absorbed in the U_3O_8. In order to obtain the effective thickness for fission fragments it was necessary to correct for the difference in range between fission fragments and particles of energy 4.75 Mev. It has been shown by Rossi and Staub (LA-1004) that the detection efficiency of a counter for α-particles is found by

$$F(B) = 1/2 \left[1 - \frac{T}{2(R_o - R_b)} \right] \qquad (2)$$

where T = thickness of foil

R_o = range of α-particles in the foil

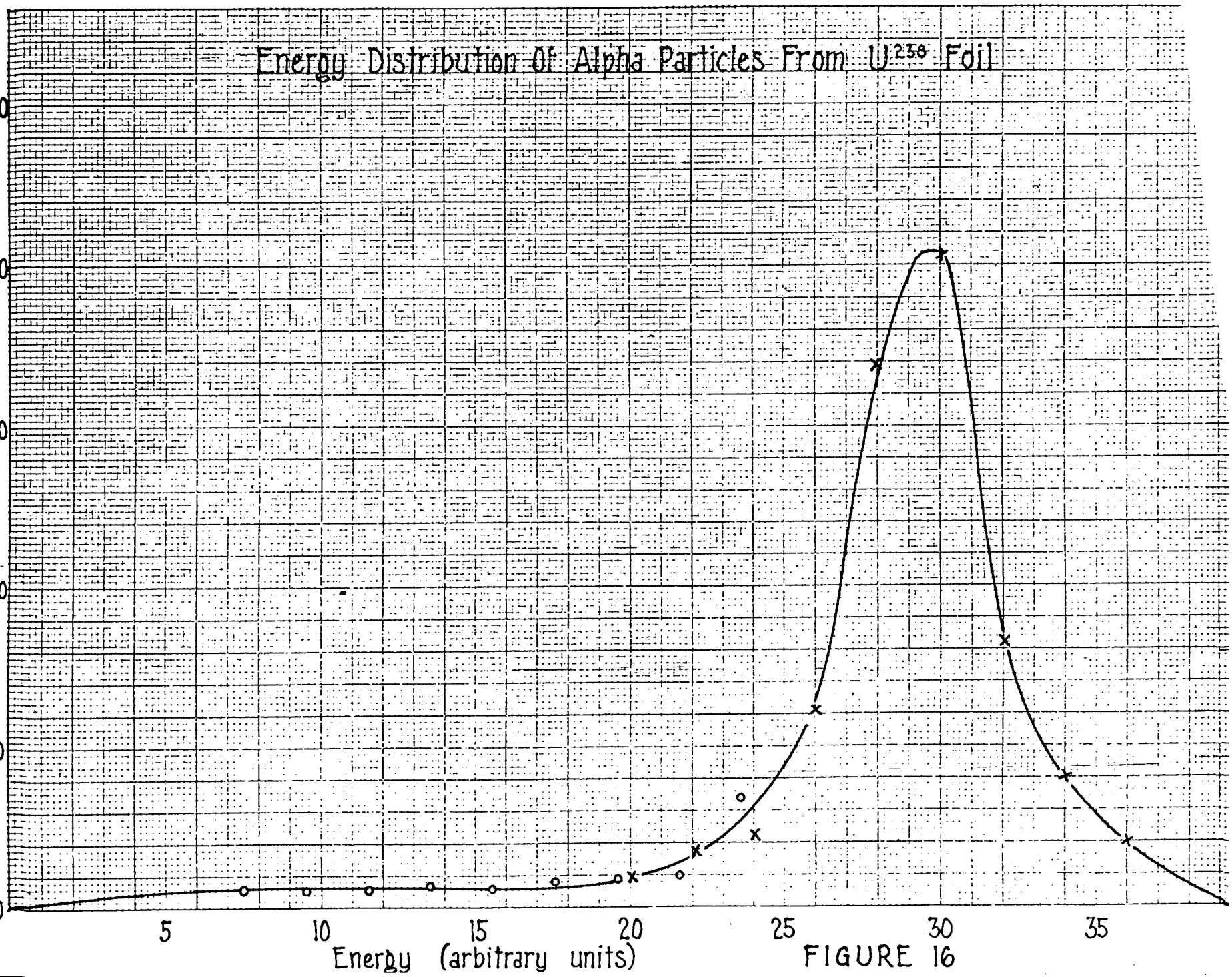

FIGURE 16

APPROVED FOR PUBLIC RELEASE

R_b = range of particles equal to the bias energy B and $T \leq R_o$.

In our cases the bias energy B is zero since we extrapolate all our curves to zero. We then have:

$$F(B) = 1/2 \left[1 - \frac{T}{2R_o} \right] \qquad (3)$$

For fission fragments the formula is of course:

$$F(B) = 1 - \frac{T}{2R_o} \qquad (4)$$

where R_o = range of fission particles.

With the aid of the above formulae and by taking the mean range of fission particles to be 10 mg/cm^2 in U_3O_8 and the range of alpha particles of energy 4.75 Mev to be 11 mg/cm^2 in U_3O_8 a correction is obtained which, when applied to the effective thickness of U_3O_8 for 4.75 Mev alphas, gives the effective thickness of U_3O_8 for fission fragments. This correction is 0.4%; i.e., the effective thickness of U_3O_8 for fission fragments is thus 0.4% less than for 4.75 Mev alphas. The effective average thickness of the U foils for fission fragments then turns out to be 0.641 mg/cm^2 and it is this value, multiplied by 12, which appears in the cross-section formula given below as Eq. (6).

As a check on the method for determining the thickness of the U^{238} from alpha activity, a foil was

counted and the U^{238} was then separated by R. W. Potter using an ether extraction method. This uranium was then weighed. The weight obtained in this manner coincided with the weight deduced from the specific activity to well within the accuracy of the chemical separation method, which accuracy was about 5%.

An initial difficulty experienced in this experiment concerned fissions produced in the fission counter by background neutrons, i.e., neutrons arising from reactions produced when deuterons strike either the cyclotron dees, the sides of the cyclotron tank, the beam collimating diaphragms or the target chamber windows. It was found possible to eliminate practically all neutrons with energy over the fission U^{238} fission threshold by shielding the cyclotron tank proper with water and paraffin. Also the slow neutrons which arose due to this process outside of the shielding were not sufficient to produce appreciable fissions in the small amount of U^{235} contained in the U^{238} foils (U^{235} was present to only 1 part in 3300). The background due to the collimating diaphragms was considerably reduced by making the diaphragm of gold. It was found that gold has only about 0.3 the neutron background of brass, for example.

The target chamber was originally used with

mica windows at all ports. The neutron background was of course chiefly due to the front and rear windows which had a combined thickness of about 5 mg/cm^2. It was found during the course of the experiment that a window of .0003" tantalum produces only 0.386 the neutron background of a 2.5 mg/cm^2 mica window and a tantalum window was accordingly substituted for the mica window at the exit port of the target. The mica window was retained at the entrance port on the basis of scattering considerations.

Even after all the above improvements were made, there were produced about 1000 background fissions in the chamber for every fission produced by a neutron in real coincidence with a He^3 entering the He^3 counter.

VI. PROPORTIONAL COUNTER

Fig. 17 shows the proportional counter used in this experiment. It is of more or less conventional design. Several special precautions were, however, taken in order to eliminate possible α-particles which might result from an n, α reaction in the glass insulator; a shield of Poly T.F.E. was placed around this insulator. All parts of the counter were also carefully decontaminated in dilute HNO_3 before assembly.

The central electrode made of 10 mil Kovar wire served as the high voltage and collection electrode, the signal being taken off through a 5000 volt .0001 MF condenser. The counter was operated with argon at pressures ranging from 20 cm to 70 cm of Hg and at voltages ranging from 500-2000 volts. The rise time of the pulses was $\sim$ 1.1μs and the pulse width was $\sim$ 2-3 μs.

Fig. 18 is a family of gas amplification curves. The counter was operated with a gas amplification of $\sim$10.

The resolution of the proportional counter was determined by obtaining the energy distribution of monoenergetic alphas produced by a thin plutonium foil under the same conditions as prevailed during the counting of He^3 particles, with the single exception that there was only one mica window between the particles and the gas in the counter - namely, the counter window.

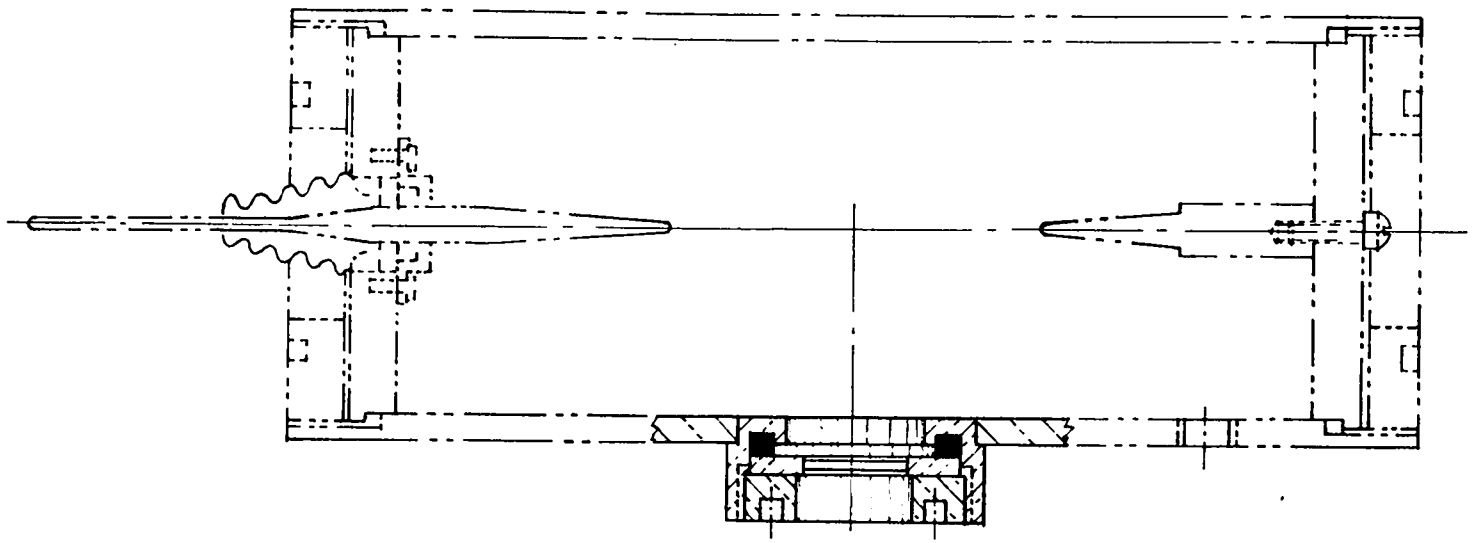

FIGURE 17

Proportional Counter

APPROVED FOR PUBLIC RELEASE

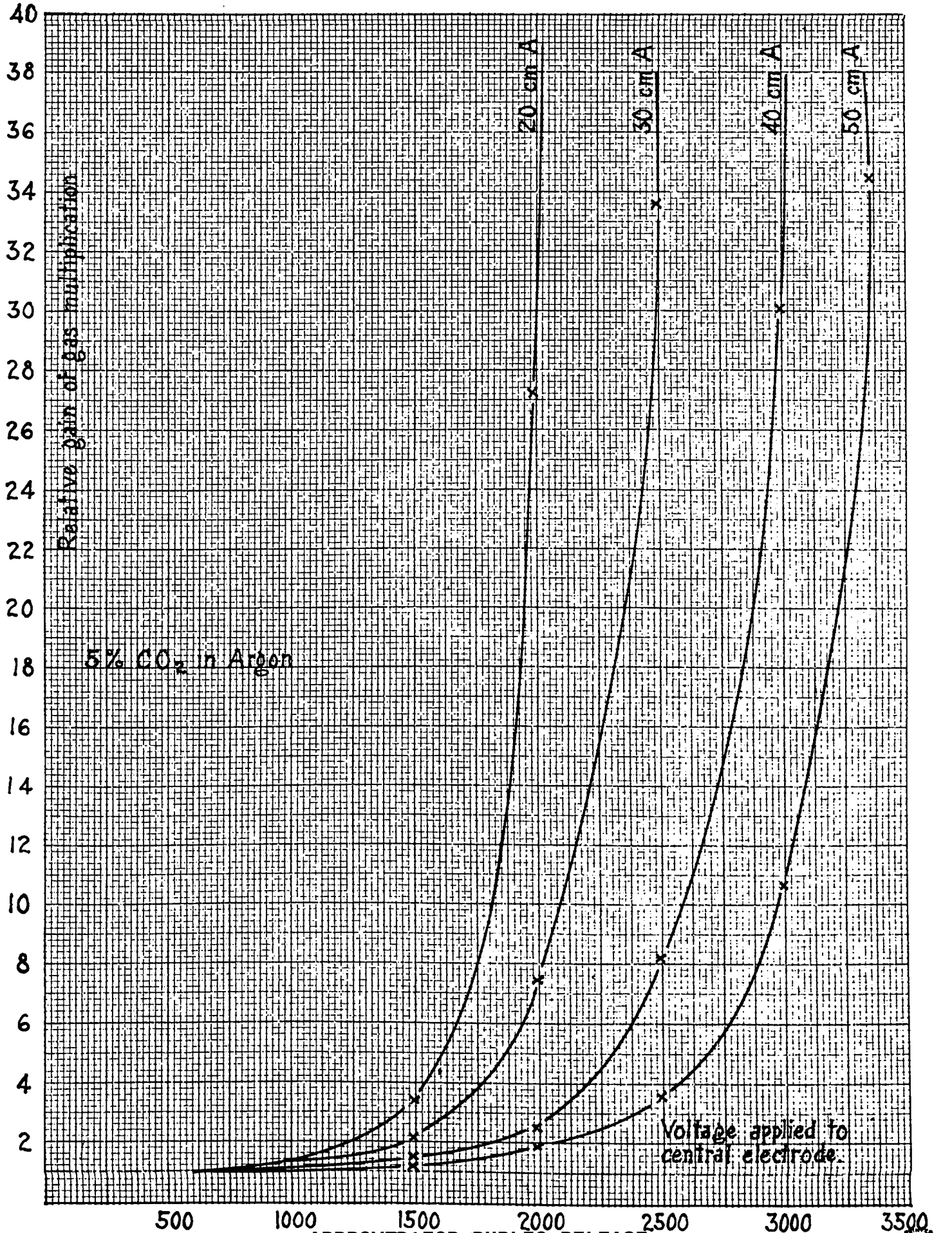

FIGURE 18

Under these conditions the width at half-maximum of the energy distribution of the plutonium alphas was 3.5%.

A number of background difficulties were experienced when first the counter was tried. The background difficulties fell into two categories, gamma-ray background and particle background. The gamma background was sufficiently reduced by encasing the counter in 2" of lead. The other major source of background, that due to ionizing particles, resulted from deuteron reactions in the mica windows of the gas target which, during the initial set-up, the proportional counter was able to see and from recoil nuclei scattered by high energy neutrons. The former difficulty was successfully eliminated by use of the target arrangement shown in Figs.21 and 22. The latter difficulty, the considerable background produced by scattering of the large neutron fluxes produced by energetic deuterons upon being stopped, was sufficiently decreased by the methods described in the preceding section.

Another source of background consisted of voltage breakdowns inside the counter. These were almost completely eliminated by applying over-voltage on the counter and allowing it to "cook" for 5 minutes.

Since the He^3 particles essentially monitored our neutron flux, it was necessary to know that the

particles counted as He^3 particles did not include scattered deuterons, protons, and tritons from the $D(D,H^3)H^1$ reaction or recoil nuclei from the neutron background. Since the rate of energy loss per cm path of D, H^1, and H^3 particles is less than that of He^3 particles, it follows that if one uses absorbers (when necessary) in front of the proportional counter and a pressure in the proportional counter such that the He^3 particles are just stopped inside the proportional counter, they will give up more energy and hence produce higher pulses than any of the other particles mentionad whether they be wholly or partially stopped in the chamber. Since the energy of the He^3 particles at any angle with respect to the deuteron beam could be calculated from the deuteron energy and the Q of the reaction, it was possible to always predict the amount of absorber necessary in front of the proportional counter together with the amount of pressure required in the counter to just stop the He^3 particles inside the counter. These predictions were in all cases borne out experimentally, which was an additional criterion for establishing the fact that the particles being counted were actually He^3 particles. This permits one to bias against protons, deuterons, and tritons. By making a background run with H^1 in the target rather than D^2, it was determined that particles

of mass >3 (for example argon recoil nuclei) gave very few if any pulses in the energy region of the He^3 pulses, and even these background counts were corrected for.

Fig. 19 shows the energy distribution of the He^3 particles obtained from the $D+D \rightarrow He^3+n$ reaction using the above counter at 39.7° with respect to the incident deuteron direction. Although the number of He^3 particles counted served to define the number of neutrons entering the fission counter and hence the neutron flux, it was not necessary to count all He^3 particles entering the proportional counter. This fact was taken advantage of by setting the bias at Point B, for example, and counting all He^3's with energy greater than this. By so doing, the background correction was reduced to approximately 1%. In order to correct for this background, the following procedure was used: The background was appropriately extrapolated as shown by the dotted line in Fig. 19. An aid to this extrapolation in the higher energy region (from Point B up) was the determination of the background with H^1 instead of D^2 in the target. A curve was then constructed of the number of background counts/unit current vs. total counts per unit current for a sufficient number of bias settings. All runs were then corrected with the appropriate correction factor.

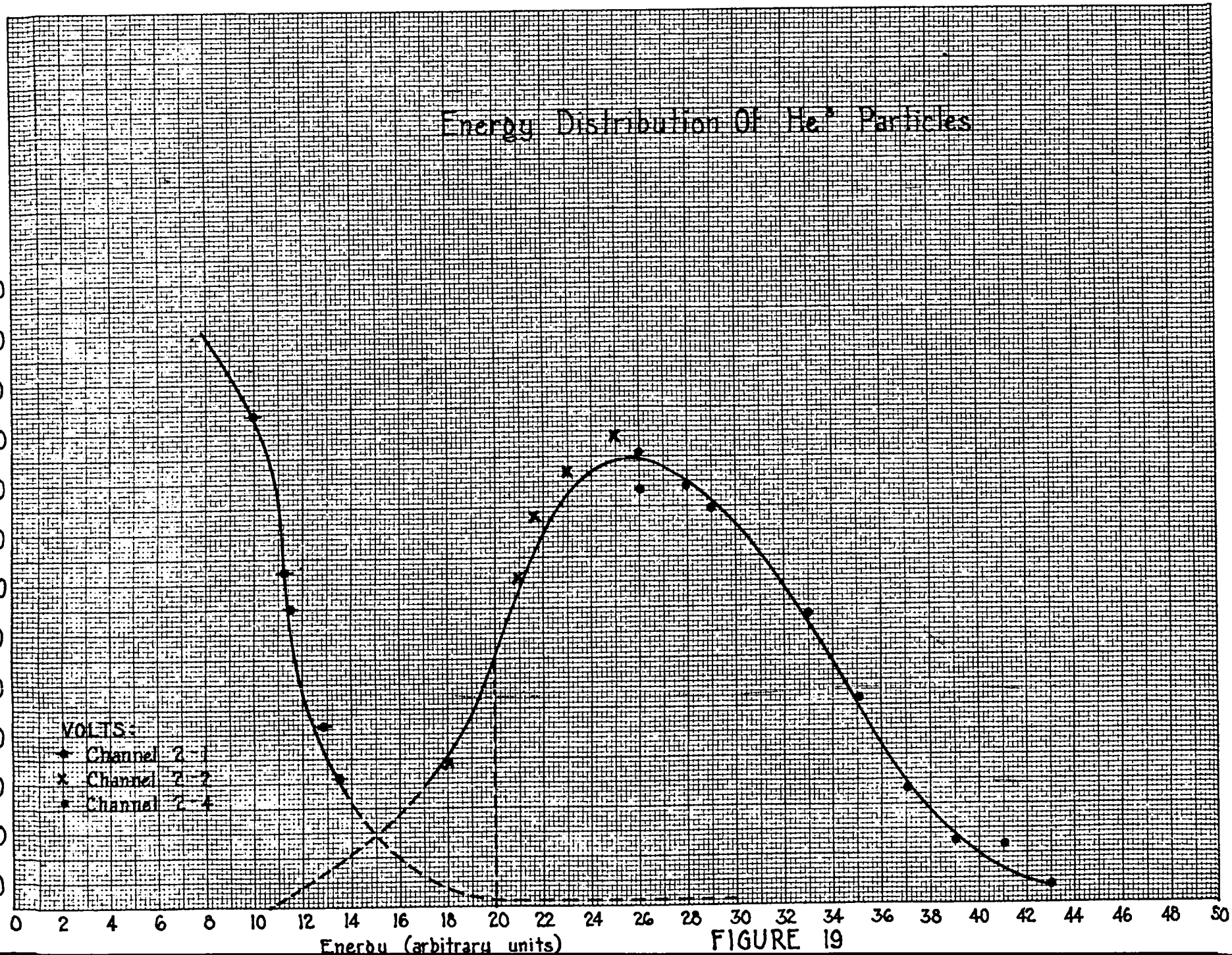

FIGURE 19

APPROVED FOR PUBLIC RELEASE

It has now been shown how the three essentials of any cross-section measurement were accurately determined; namely, the flux of bombarding particles (in our case neutrons whose flux was determined by counting the coincident He^3 particles), the amount of material intercepting this particle flux and the number of reactions produced (in our case, this of course involved determining the number of fission particles liberated with energy sufficient to penetrate the foil of active material). The following equation determines the fission cross-section from these three quantities as determined from the above evaluations.

$$\frac{\text{No. of fissions}}{\text{Unit Time}} = \frac{F}{\text{Unit Time}} \times \frac{\sigma \times A \times n \times T \times 10^{-3} \times 6.023 \times 10^{23}}{238} \qquad (5)$$

where the symbols have the following meaning:

$F =$ number of neutrons/cm^2 in coincidence with He^3's

$\sigma =$ cross-section per U^{238} nucleus

$A =$ average area of foils exposed to neutron beam

$n =$ number of foils

$T =$ average thickness in mg/cm^2 of U^{238} in foils corrected as outlined above.

Since $F = N/A$ where $N =$ total number of neutrons in coincidence with He^3's which enter the proportional counter

We have

[redacted]

$$\text{No. of Fissions} = \frac{N}{A} \times \frac{\sigma \times A \times n \times T \times 10^{-3} \times 6.023 \times 10^{23}}{238}$$

and

$$\frac{\text{No. of fissions} \times 238}{N \times n \times T \times 6.023 \times 10^{20}} = 5.14(\pm 1.3\%) \times 10^{-20} \times \frac{\text{No. of real fissions}}{N} \qquad (6)$$

where the number of fissions are given by the number of real coincidences corrected as outlined above and N is given by the number of He^3's counted, also appropriately corrected for background.

[redacted]

VII. NEUTRON ABSORPTION CORRECTION

Since only fission in coincidence with neutrons which are emitted in a collimated cone are counted, one does not have to worry about neutrons scattered into the counter by the walls of the reaction chamber, etc. However, it is necessary to correct for those neutrons in the defined cone which would have passed through the counter but which were absorbed or scattered out of the beam by the intervening material. Therefore, the walls of the targets and the scattering chamber in the path of the beam were milled down so that there was only 1/16" of brass and 1/8" of steel between the counter and the target gas. (Figs. 2, 3, 21, and 22). The absorption correction for this material and also the walls and plates of the fission counter was determined experimentally.

Absorption runs were made using the 10.5 min. activity of a $Cu^{63}(n, 2n)Cu^{62}$ detector. It had been shown previously that most of the activity of this threshold detector was due to neutrons from the $D(d,n)He^3$ reaction in the deuteron target. The background found by substituting hydrogen for deuterium in the target was about 10%. The experimental set-up is indicated in Fig. 20. This experiment gives absorption and inelastic scattering of neutrons from above the threshold

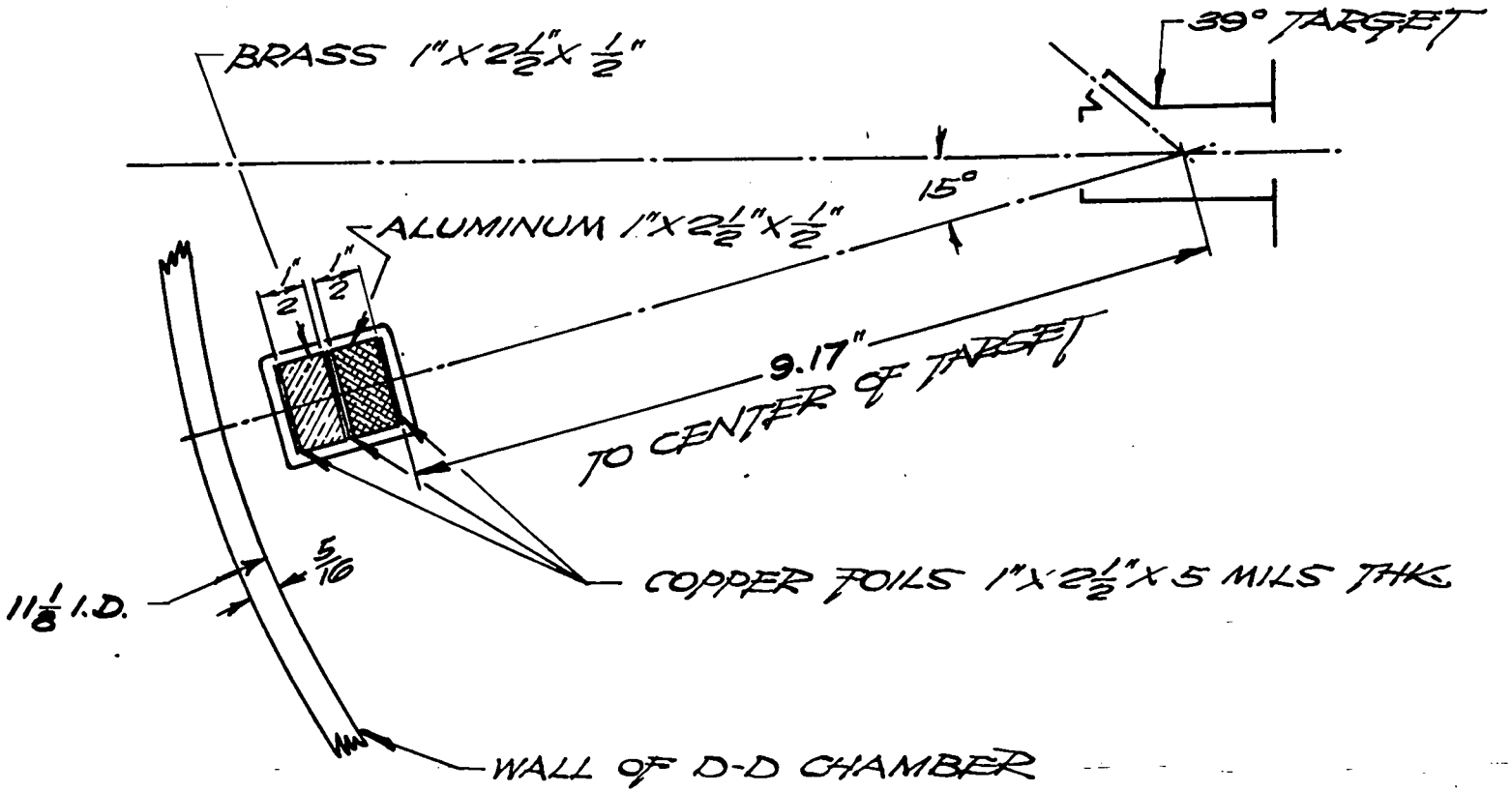

FIG. 20

SET UP FOR DETERMINING NEUTRON ABSORPTION CORRECTION

APPROVED FOR PUBLIC RELEASE

$11<E_n<12$ Mev. (A report on $Cu^{63}(n,2n)Cu^{62}$ reaction is forthcoming). Copper foils 1"x2½"x5 mils thick were used as detectors. The copper foils were sandwiched between plates of the material, the absorption of which was being studied. The group of absorber and foils were covered by 30 mil cadmium to reduce slow neutron activity. The front foils monitor the neutron beam. The ratio between activity of the back foil and the foil in front of any absorber gives the neutrons absorbed or scattered from the beam by that absorber, after a slight correction for solid angle is applied. Second order corrections due to neutrons back-scattered into the front foils were not applied for the evaluation of this correction factor.

The deuterium gas of the targets was bombarded for about 20 minutes by the cyclotron deuterons and then the foils were removed and counted in glass-walled geiger counters. Each sample was counted about 5 times in each of three counters, so that 3 decay curves for each sample were obtained. The 10.5 minutes activity was well resolved. A summary of the results is in Table I. The error is obtained from the spread in activities of the three counters and hence is only the counting error.

TABLE I

Absorber	Thickness	N_b/N_f Activity Back Foil / Activity Front Foil	Absorption Factor = Log N_f/N_b
Brass	1/2"	.86 ± .02	.15 ± .02
Steel	1/2"	.87 ± .02	.14 ± .02
Aluminum	1/2"	.99 ± .02	.01 ± .02

One can make an estimate of the absorption factor for iron from data in the literature. The total cross-section for iron by transmission experiments is given as 2.8 ± 0.3 barns (Rev. of Mod. Phys. 19, #4, 275, (1947)). Since most neutrons scattered into the forward direction would be detected in our experiment, one should subtract the inelastic scattering in the forward direction from this value. A rough estimate of this scattering cross-section can be obtained from Barschall and Landenburg (Phys. Rev. 61, 129, 1942) which was measured at 2.5 Mev and is 0.9 ± .2 barns. The absorption factor calculated from these values [2.8 (± 0.3) - 0.9 (± .2) = 1.9 ± 0.4] barns is .20 ± .04, which is to be compared with our measurement of .15 ± .02. They agree within the limits of error, even though the estimates involve measurements made at somewhat different energies. Barschall and Landenburg also find that the absorption of aluminum is somewhat less than that from iron, in agreement with Table I.

The $Cu^{63}(n,2n)$ determination of absorption of neutrons from the beam agreed within the limits of error with a determination which was made using the fission counter as a neutron detector. This experiment involved taking runs on the real coincidence fissions per He^3 particle with and without additional absorbers being present. The statistical errors and other errors were too large, however, to warrant using this latter method to evaluate the absorption correction.

Using the data given in Table I, one can calculate the neutron absorption correction which must be applied to the data to obtain the U^{238} cross-section. Table II gives the thickness of each material between the neutron source and the average plate of the fission counter during the runs for the determination of this cross-section.

TABLE II

Material	Thickness	$\underline{A}$ Absorption Factor from Table I
Steel	.125"	.035 ± .005
Brass	.076"	.023 ± .003
Aluminum	.312"	.006 ± .012
		ΣA_i = .064 ± .013

This indicates about a 6% correction must be applied to the data to allow for neutrons absorbed or scattered out of the beam.

VIII. EXPERIMENT

The procedure followed in preparing for and carrying out the determination of the cross-section at a certain neutron energy is as follows:

A. Install and line up the suitable gas target.

B. Determine the spread and position of the deuteron beam.

C. Determine the energy of the deuteron beam.

D. Install suitable diaphragms in the proportional counter and target and line up the fission counter.

E. Calibrate amplifiers, etc.

F. Adjust proportional counter voltage and/or gain to give to give correct amplitude He^3 peak.

G. Make runs of about 1/2 hour duration and record fissions, He^3's counted, and coincidences.

H. Make runs for resolving time determination.

I. Repeat energy measurements from time to time.

A. The gas targets used in this experiment are illustrated in Fig. 21 and Fig. 22. Table III gives the thickness of mica on the windows used to obtain each point. A gold diaphragm 30 mils thick with a 0.466" diameter hole is fastened in front of the target to

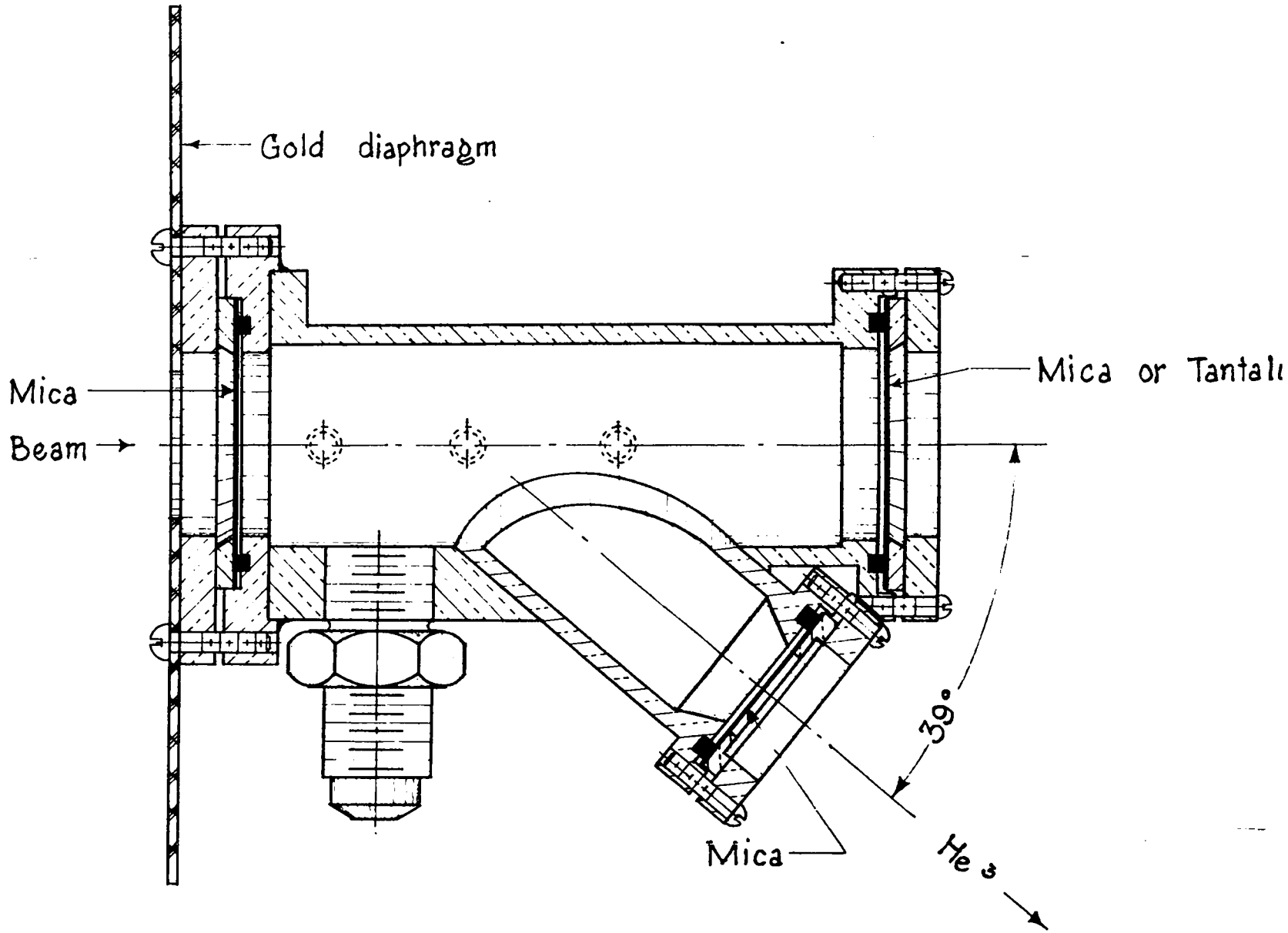

39° GAS TARGET
FIGURE 21

APPROVED FOR PUBLIC RELEASE

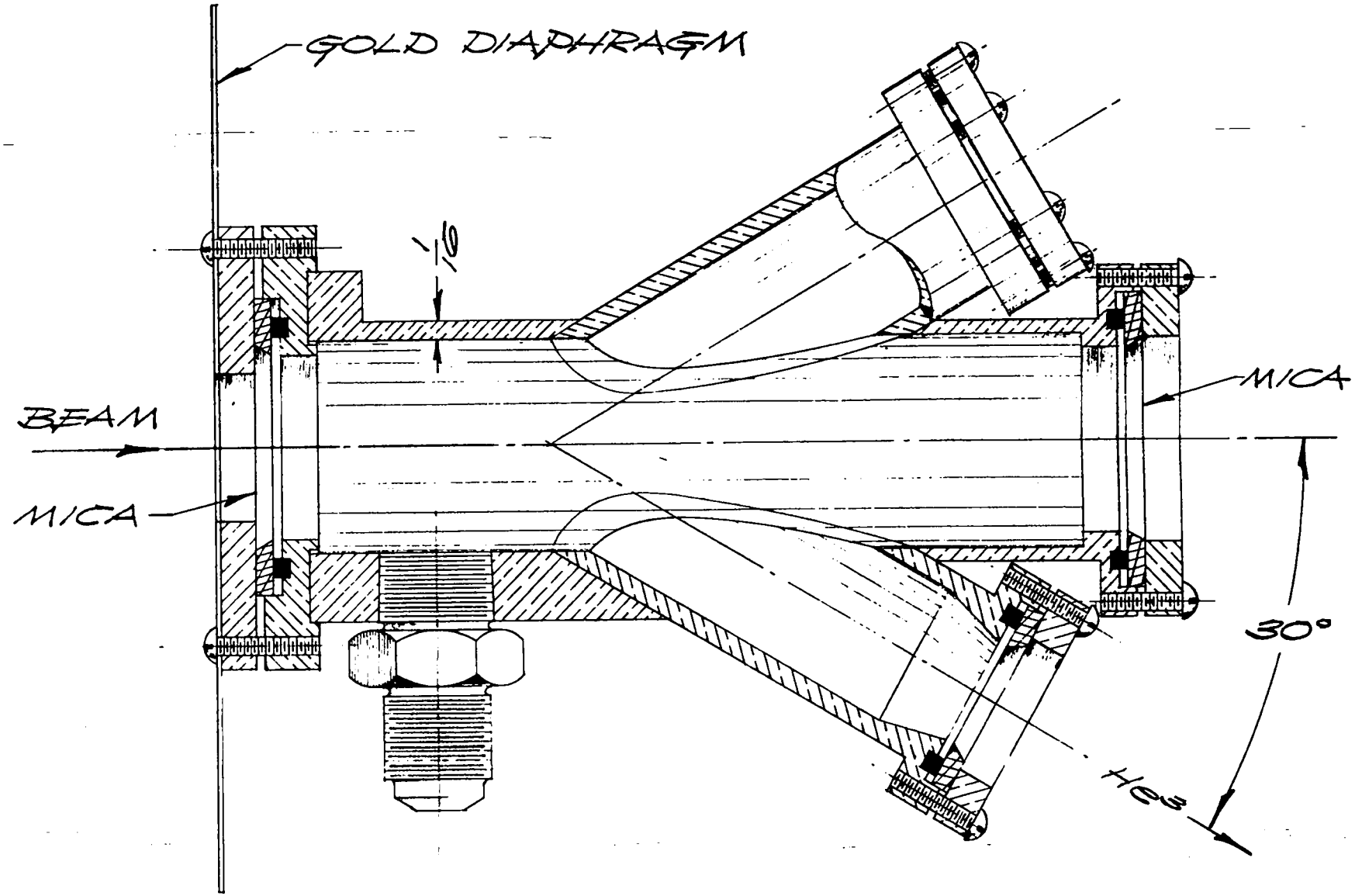

30° GAS TARGET
FIG. 22

APPROVED FOR PUBLIC RELEASE

APPROVED FOR PUBLIC RELEASE

SERIES	ϕHe^3	DIAPHRAGM FOR He^3 PARTICLES: TARGET	DIAPHRAGM FOR He^3 PARTICLES: PROPORTIONAL COUNTER	THICKNESS OF WINDOWS IN TARGET: ENTRANCE	THICKNESS OF WINDOWS IN TARGET: EXIT	THICKNESS OF WINDOWS IN TARGET: He^3 PORT	ENERGY OF DEUTERON BEAM MEV	HORIZONTAL SPREAD He^3 BEAM $\Delta\phi He^3$	VERTICAL SPREAD He^3 BEAM $\Delta\zeta He^3$	CENTER OF NEUTRON BEAM ϕn	HORIZONTAL SPREAD NEUTRON BEAM $\Delta\phi n$	VERTICAL SPREAD NEUTRON BEAM $\Delta\zeta n$
1	40.7°	3/16"x3/8"	3/16"x3/8"	2.82 mg/cm² mica	2.60 mg/cm² mica	1.30 mg/cm² mica	10.20	±2.28°	±3.8°	55.6°	±5.7°	±4.8°
2	29.7°	1/8"x1/4"	1/8" Dia.	2.60 mg/cm² mica	2.2 mg/cm² mica	2.0 mg/cm² mica	9.86	±2.10°	±2.3°	82.3°	±5.0°	±4.6°
3	39.7°	9/32"x3/8"	3/16"x3/8"	2.7 mg/cm² mica	.0003 mil Tantalum	1.4 mg/cm² mica	10.75	±2.15°	±3.80°	56.00°	±5.3°	±4.8°

TABLE III

limit the beam. After installing the windows and testing them under pressure, one lined up the target. The back plate, slits, and Faraday cage were removed from the energy measuring section so that one could sight a telescope along the 0 - 180° reference line of the D-D chamber, as established by dropping a plumb bob from the graduated ring (Fig. 4). The target was moved on its platform and rotated until it was lined up on the line of sight. By use of a surface guage the height of the target was adjusted to that of the beam, which came 5-23/32" above the base of the chamber. It was estimated that the alignment could be accomplished to about 1/64".

B & C. The procedure followed in determining the spread and position of the beam has been described in Section II. The maximum angular spread of the beam was limited to $\pm$ 0.63° by a gold diaphragm in the 6" tube from the focus magnet. The energy of the deuteron determination has also been described in Section III.

D. From the energy and angular spread of the beam one calculates the diaphragms for the proportional counter and He^3 exit tubes of the target so that the associated cone of neutrons falls well within the U^{238} foils of the fission counter, the last foil of which subtends a cone of total included angle of 12.1°. The results of these calculations are given in Table III.

By having the cone of neutrons somewhat smaller than the cone of the fission counter, one can allow for small errors in aligning the equipment and in measuring the deuteron energy. For example, a 2% shift in deuteron energy corresponds to a shift of the neutron angle by 0.36° when the He^3 angle is 39°.

Next, the center of the fission counter is lined up on the correct angle corresponding to the angular setting of the proportional counter. This is done by establishing a line with a straight edge which is directly over the calculated angle as determined by the graduated ring within the D-D chamber. When the fission counter is rotated to the correct position the reading of the angular scale on the track is taken. Thus, for each setting, the track is calibrated against the graduated ring. By use of a straight edge and a scale, the height of the fission counter is adjusted to be the same as that of the target and proportional counter. The angular settings of the fission counter together with that of the proportional counter for the various series of runs is given in Table III.

The calibration of the amplifiers and adjustments of the discriminator bias of the coincidence circuit are described in Sections V and VI. Before a run or series of runs one checks and records the gas

pressure in the target, the proportional counter, and the fission counter. Then the high voltage to the counters is switched on. With a cyclotron beam one adjusts the high voltage for the proportional counter to give the He^3 pulses of the desired amplitude as described in Section VI.

G. Now one is ready for the experiment. After a fairly steady cyclotron beam is obtained, one records the readings of the proportional counter scaler, the fission scaler, the coincidence scaler, and the current integrator scaler, together with the time at which the electronic apparatus is switched on. The beam is held as steady as possible for 1/2 hour and the experimentor records any intervals of time the beam is off. This off time is added to the length of the run at the end. At the end of 1/2 hour of beam the time and the readings of the above scalers are again recorded.

H. From time to time, the resolving time of the coincidence circuit is determined experimentally. Runs of 1/2 hour duration are made similar to the one described above, except that the fission counter is rotated to such an angle that no neutrons associated with the He^3 particles can pass through it. Since for such runs all coincidences are accidental, one can calculate the resolving time from the simple relationship.

$$Ca = \frac{(N_{He3})\,(N_f)\,(\Delta\tau)}{\Delta t} \qquad (7)$$

where $Ca =$ accidental counts obtained during interval

$N_{He3} =$ He^3 counts obtained

$N_f =$ fission counts obtained

$\Delta\tau =$ resolving time

$\Delta t =$ time of observation.

Since the accidental rate is determined by such runs spaced between the real runs, variations of cyclotron beam, etc., should average about the same for both sets of runs, so that the evaluation of the accidental counts during the real runs should be rather valid. The experimentally determined resolving times for all series of runs are recorded in Table IV.

TABLE IV

Series	E_n Neutron Energy Mev	τ Experimental Resolving Time (sec)	C_r/N_p Average of Series	C_r/N_p Corrected for Neutron Absorption	C_r/N_p Corrected for Fission Counter Bias	σ_{28} Barns
1	8.8 ± 0.5	2.23 ± .12x10^{-6}	20.8 ± 2.0x10^{-6}	22.2 ± 2.2x10^{-6}	22.7 ± 2.2x10^{-6}	1.17 ± .11
2	5.8 ± 0.4	1.87 ± .09	12.1 ± 2.5	12.9 ± 2.7	13.2 ± 2.7	0.68 ± .14
3	8.9 ± 0.5	1.90 ± .12	18.7 ± 2.3	20.2 ± 2.4	20.2 ± 2.4	1.04 ± .12

APPROVED FOR PUBLIC RELEASE

RESULTS

Each series of runs required about 15 separate runs of 1/2 hour each. The deuteron beam current was so adjusted as to give about equal number of real coincidences and accidentals. The data for this series of runs is given in Appendix III. Figs. 23, 24, and 25 show graphically how the number of real coincidences per He^3 particles for the sequence of runs varies. The points are plotted in the order in which they were taken. The represented error is calculated from the counting errors of the total coincidences and that of the accidentals. Thus, the quantity plotted for a run of Δt duration in which there are C total coincidences, N_{He3} He^3 counts, N_f fission counts is

$$\frac{Cr}{N_{He3(corr)}} = \frac{C-\frac{(N_{He3})(N_f)\Delta\tau}{\Delta t}}{N_{He3(corr)}} \pm \frac{\sqrt{C+\frac{(N_{He3})(N_f)\Delta\tau}{\Delta t}+\left(\frac{N_{He3}\,N_f\,\epsilon\tau}{\Delta t}\right)^2}}{N_{He3(corr)}} \qquad (8)$$

where $\Delta\tau$ is the resolving time and $\epsilon\tau$ is its standard error as determined from the runs on resolving time. That the data and the errors are statistically significant is indicated by the way the points fall around their mean. About 2/3 of the points lie within their standard error of the mean in agreement with the principles of

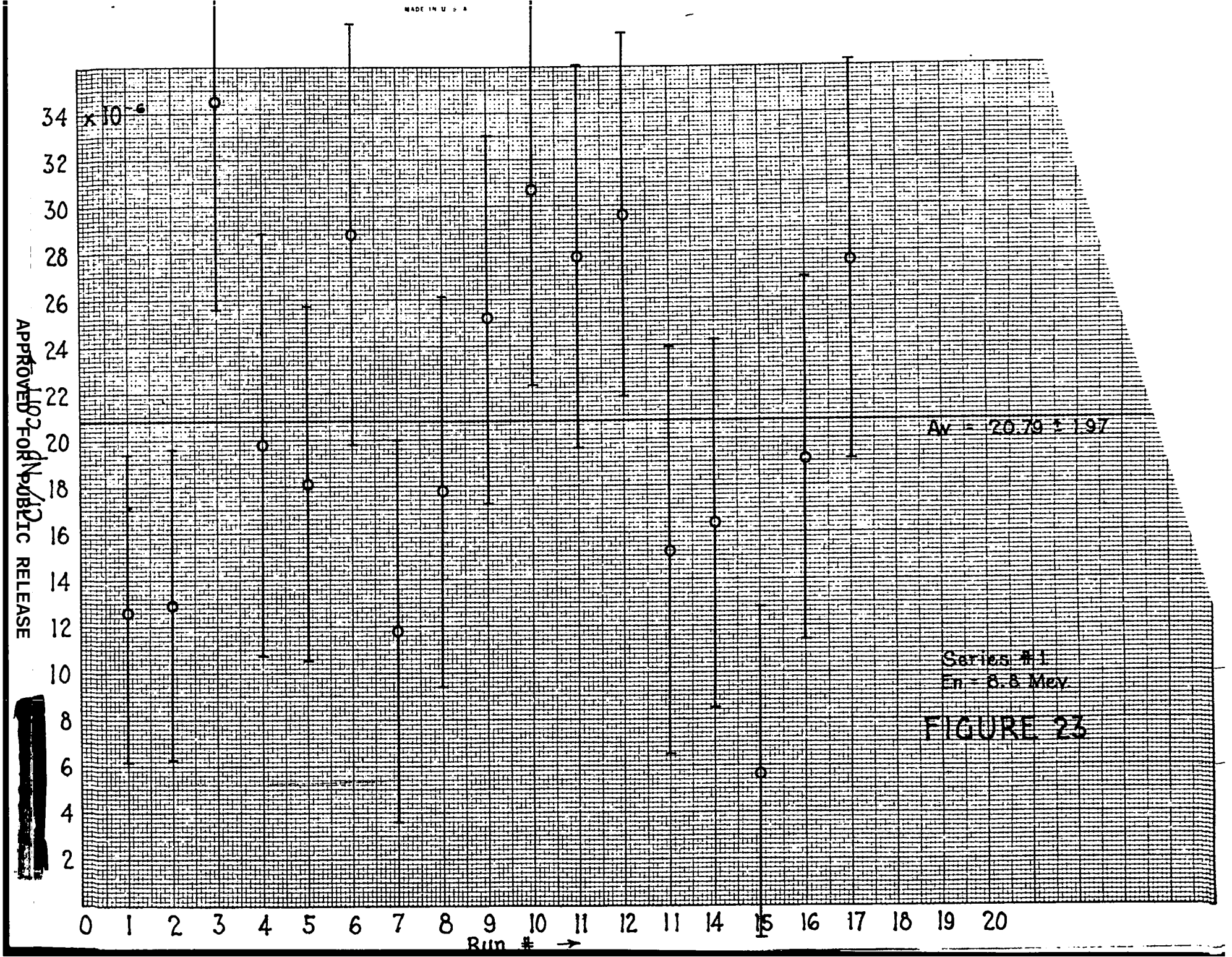

FIGURE 23

APPROVED FOR PUBLIC RELEASE

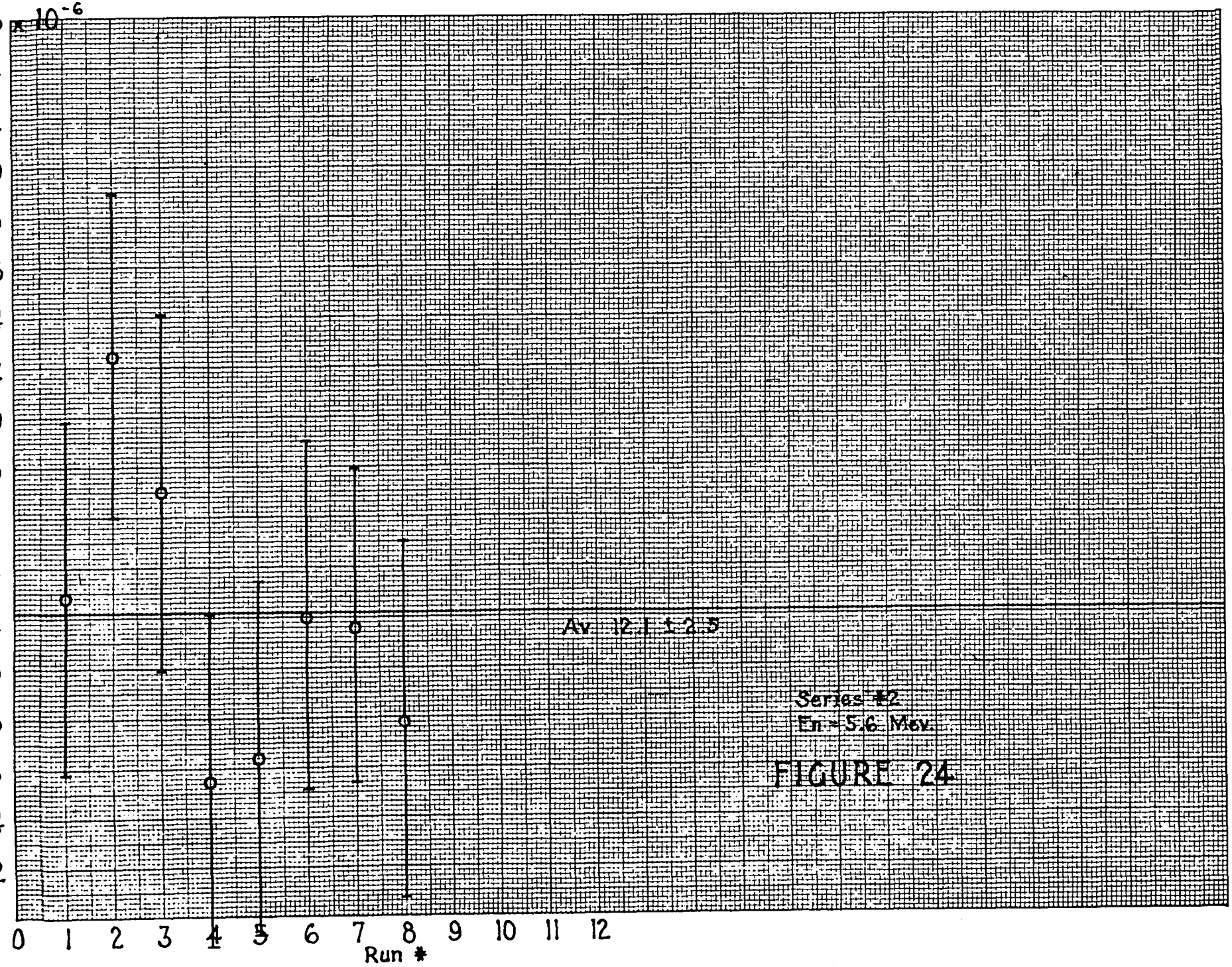

FIGURE 24

APPROVED FOR PUBLIC RELEASE

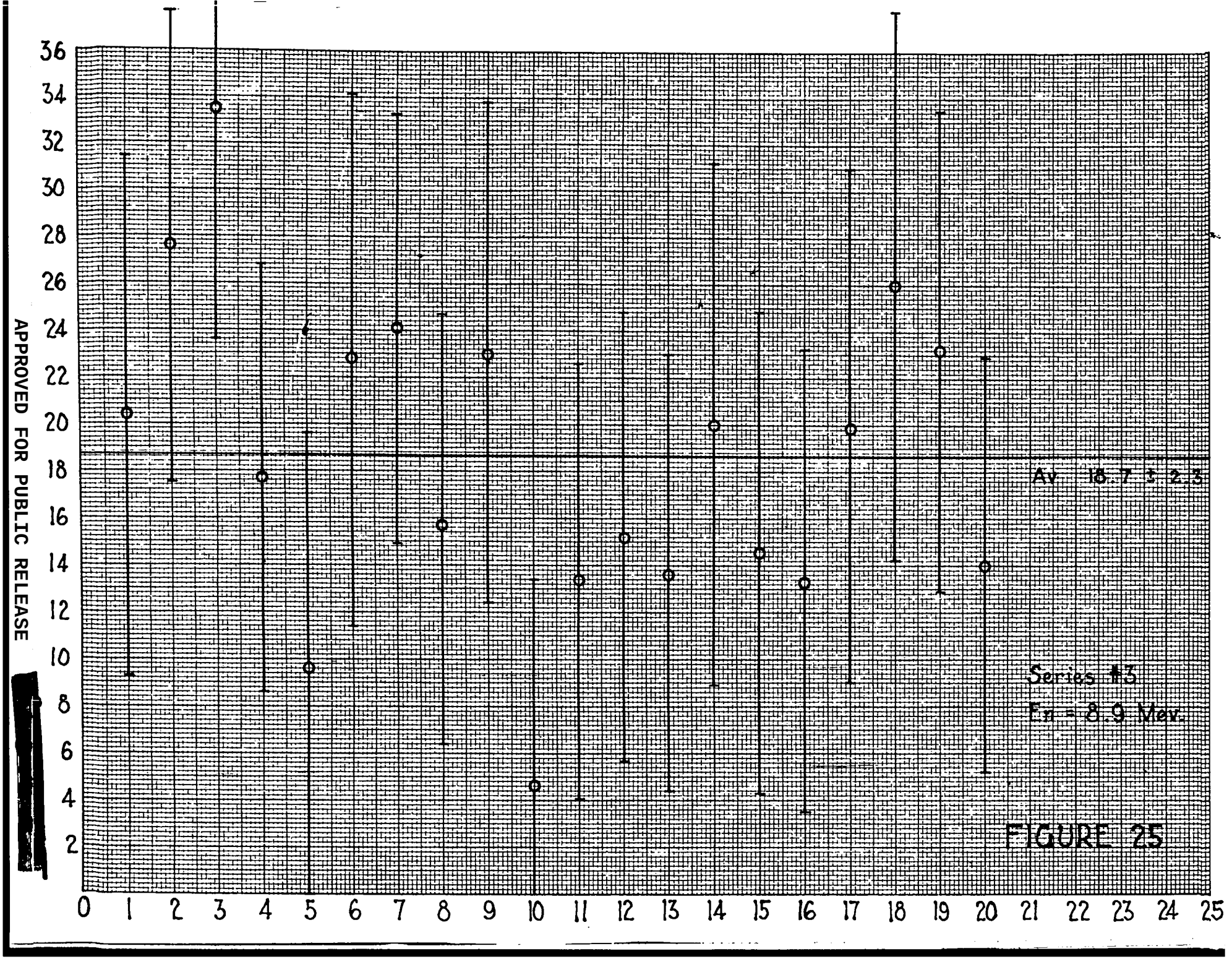

FIGURE 25

APPROVED FOR PUBLIC RELEASE

probability. The data does not indicate a significant trend with order or runs.

As an example of the calculation of the result of a 1/2 hour run, consider the data for the first point of Fig. 25. From Appendix III, Series 3, the recorded data was as follows:

Δt = length of run = 30 min.

N_f = fission counts = 32,350

N_p = He^3 proportional counts = 752000

C = coincidences counts = 41

Using Equation (7) and the resolving time for Series #3 runs (TABLE IV) which is $\Delta\tau = 1.90 \pm .12$ μs one has

$$C_a = N_{He3}\, N_f \frac{(\Delta\tau)}{\Delta t} = 25.7 \pm 5.2$$

where the error is essentially the square root of the number of accidental counts. This is increased slightly by the error of the resolving time.

The real coincidences then are:

$$C_r = C - C_a \pm \sqrt{C + \varepsilon_a^2} = 15.3 \pm 8.3$$

By the method described in Section VI it had been determined that for this run a fraction (.994) of the counts of N_p are due to He^3

So $N_{He3} = 0.752 \times 10^6 \times 0.994 = 0.748 \times 10^6$

Thus:

$$\frac{C_r}{N_{He^3}} = \frac{15.3 \pm 8.3}{0.748 \times 10^6} = (20.4 \pm 11) \times 10^{-6}$$

TABLE IV gives a summary of the data. Column 2 shows the average energy of the neutrons. The spread in energy corresponds to the width at half maximum of the energy distribution curve, and is derived from considerations of the angular spread of the He^3 due to finite width of slits and the angular spread and the energy spread of the deuteron beam. Column 4 is the mean value of the determination of the ratio of real fission coincidences per He^3 particles as taken from the data in Figs. 23-25. In Column 5, this ratio is corrected for neutron absorption by dividing by ϵ^{-A} where A is the absorption correction as discussed in Section VII. In Column 6, the data is corrected for the finite thickness of the U^{238} deposited on the foils of the fission counter as described im Section V. Column 7 gives the cross-section in barns after all corrections are applied.

In Fig. 26, the data discussed in this paper are plotted together with other determinations of fission cross-sections of U^{238}. Below 3 Mev the cross-section has been well established by a number of investigators (LA-520). The new value at 5.6 Mev agrees with previously determined values by the long electrostatic

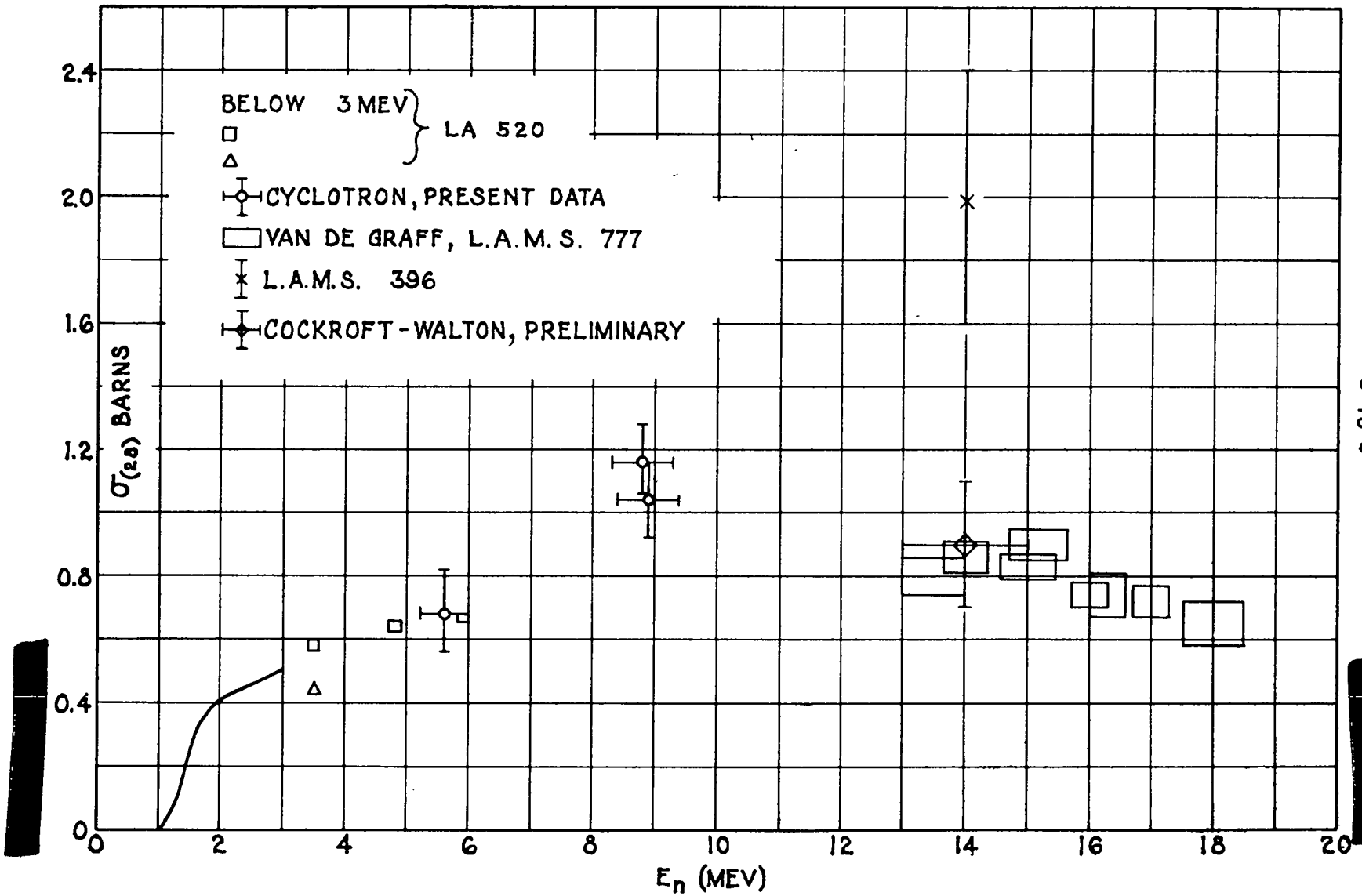

Fig. 26

APPROVED FOR PUBLIC RELEASE

generator. The new values at 8.7 and 8.9 Mev check each other and indicate that the cross-section is somewhat larger in this region than was previously supposed.

APPENDIX I

The details of the derivation of the energy equation are found in Creutz and Wilson's report. The procedure used in this experiment is as follows. Neglecting the relativity correction it is possible to rewrite the energy formula as

$$\frac{2M_o C^2 W}{C^2 A^2} = \left[1 + \left(\frac{a + b/2\ (1 - C^2A^2/8M_oC^2W)}{D}\right)^2\right]$$

Or

$$k(D) = 1 + \left(\frac{a + b/2\ (1 - 1/4k(D))}{D}\right)^2$$

Expanding:

$$k(D) = 1 + \left(\frac{a + b/2}{D}\right) - .1532\ \frac{1}{1 + \left(\frac{a + b/2}{D}\right)^2} + - - - - \qquad (9)$$

Thus k(D) may be found for any given value of D.
The energy is then given as

$$W\ (\text{Mev}) = Ck\ (D)\ (\Delta I)^2 \qquad (10)$$

where C is a constant = 87.55.

A sample family of curves is attached. The correction for a given galvanometer deflection for the zero field is given in Chart I.

Let us assume that the measured values were

D = 16.4 cm

Δ I = 113.05 milliamperes + 1 cm reading on the galvanometer

Residual field (180° turn of flipcoil) = 8cm. Then Δ I corrected would be 113.05 + 1.6 milliamperes or 114.65 ma.

From Chart I we obtain the deflection correction d_o to be 0.7 cm and the current correction to be 5 milliamperes. The final value of D is 16.4 + 0.7 or 17.1 cm and Δ I = 114.65 + 5.0 = 119.65 milliamperes.

From Chart II we find for these values an energy of 10.34 Mev. Applying the relativity correction which amounts to approximately 0.3% in the region, the final value of the energy is 10.31 Mev. This value must be corrected for target gas and windows in order to obtain the energy at the desired point where the deuterons intersect the exit cone to the proportional counter.

It should be noted that if the values a or b are changed a new family of curves must be drawn. If w, the width of the rectangular flux coil, is changed, a new value of constant C must be determined.

Procedure

1° Add do to deflection as measured.

2° Add ΔI_o to $\Delta I \pm \frac{\text{scale cm deflection}}{3.5} \times 5.6$ md.

3° Read energy on chart II.

4° Add correction for mica window and D_2 gas.

5° Add correction for relativity at 10 mev = -0.026 mev.

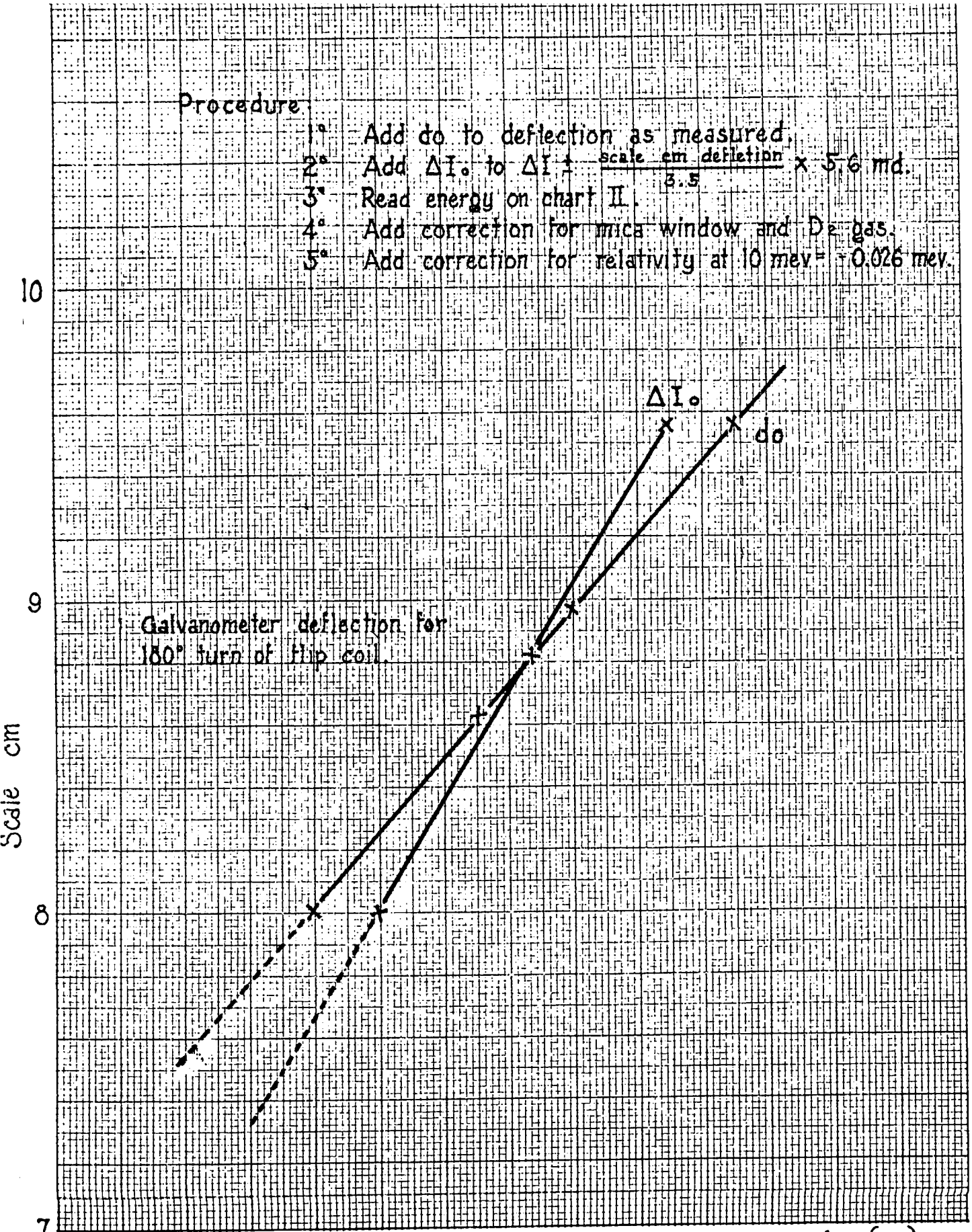

CHART II

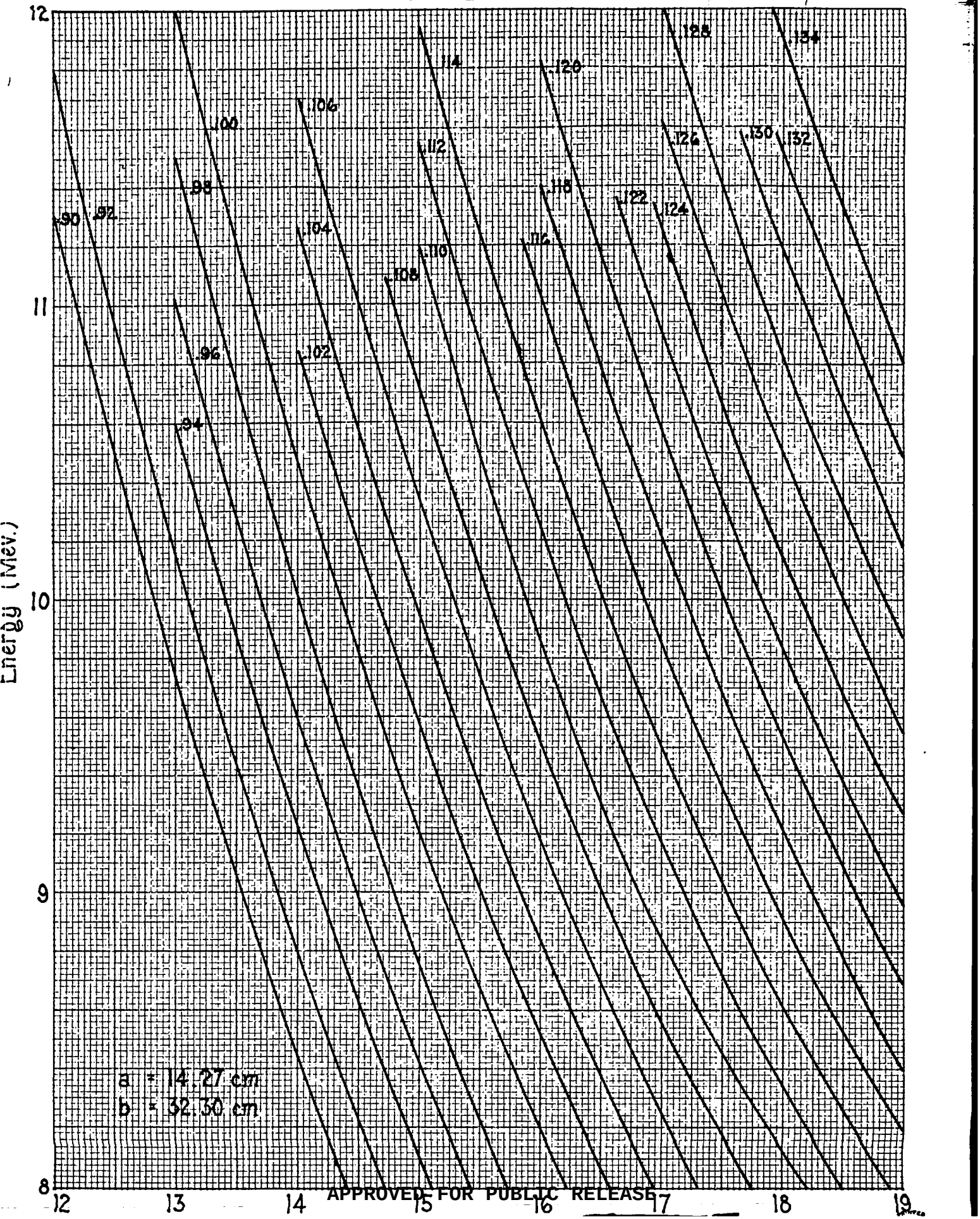

APPENDIX II

Date	Series No.	D cm	ΔI_c ma	E Mev	E Ave.	E_c
2-16-48	1	17.81	124.01	9.92	9.99	10.12
		17.66	123.75	10.04		
		17.61	122.96	9.94		
		17.61	121.81	9.92		
		17.44	122.42	10.00		
		17.41	121.73	9.95		
		17.31	121.61	10.08		
		17.31	121.96	10.10		
2-20-48	1	17.31	122.58	10.10	10.04	10.19
		17.34	122.33	10.12		
		17.36	127.60	9.98		
		17.36	121.14	9.94		
2-23-48	1	17.76	126.24	10.28	10.17	10.30
		17.71	125.30	10.16		
		17.71	124.91	10.13		
		17.53	124.53	10.18		
		17.48	123.79	10.10		
3-1-48	1	17.64	123.83	10.01	9.97	10.10
		17.44	123.01	10.00		
		17.39	122.80	9.99		
		17.39	122.04	9.89		
2-25-48	1	19.00	131.96	10.25	10.17	10.31
		18.85	132.47	10.21		
		18.85	131.28	10.05		
3-22-48	2	18.01	123.01	9.47	9.61	9.80
		17.95	122.67	9.52		
		17.90	122.51	9.52		
		17.90	122.43	9.52		
3-25-48	2	18.00	124.44	9.78	9.75	9.98
		17.95	124.41	9.78		
		17.95	124.00	9.68		
		17.83	124.00	9.74		
3-31-48	2	18.10	123.77	9.55	9.64	9.80
		17.65	121.34	9.58		
		17.45	119.96	9.58		
		17.25	119.62	9.70		
		17.20	119.76	9.79		

(continued)

[redacted]

(Appendix II, cont'd)

Date	Series No.	D cm	ΔI_c ma	E Mev	E Ave.	E_s
6-15-48	3	16.55	120.24	10.54	10.55	10.80
		16.45	120.01	10.60		
		16.55	120.00	10.50		
6-18-48	3	16.84	120.14	10.28	10.35	10.70
		16.74	119.55	10.22		
		16.59	119.31	10.50		
		16.54	118.84	10.40		
6-21-48	3	17.29	123.84	10.35	10.41	10.76
		16.99	122.44	10.43		
		16.89	121.94	10.43		
		16.87	121.33	10.38		

LA 710

[redacted]

APPENDIX III

Series #1

Run No.	Δ t Sec.	N_f Counts	N_p Counts	C Coincidences	$\frac{Cr}{N_p}$ Corr.
1	$1.800 \cdot 10^3$	$3.29 \cdot 10^4$	$1.737 \cdot 10^6$	75	$12.7 \pm 6.8 \cdot 10^{-6}$
2	1.800	2.80	1.536	59	12.5 ± 6.7
3	1.800	2.46	1.235	80	34.5 ± 9.0
4	1.800	2.165	.947	44	19.8 ± 9.0
5	1.800	2.940	1.727	94	18.2 ± 7.6
6	1.680	1.172	.747	33	28.8 ± 9.0
7	1.800	3.799	1.782	105	11.9 ± 8.2
8	1.805	3.269	1.517	88	17.8 ± 8.4
9	1.800	2.503	1.465	81	25.1 ± 7.9
10	1.800	2.055	1.180	66	30.7 ± 8.5
11	1.800	1.893	1.152	59	27.8 ± 8.2
12	2.355	1.650	1.000	45	29.6 ± 7.9
13	1.441	1.875	.997	44	15.2 ± 8.8
14	1.800	2.920	1.583	83	16.4 ± 7.9
15	1.800	1.341	.818	18	5.7 ± 7.0
16	1.744	1.428	.965	36	19.1 ± 7.7
17	1.620	1.534	.987	48	27.6 ± 8.6

APPENDIX III

Series #2

Run No.	Δt Sec.	N_f Counts	N_p Counts	C Coincidences	$\frac{Cr}{N_p}$ Corr.
1	$1.800 \cdot 10^3$	$2.105 \cdot 10^4$	$.886 \cdot 10^6$	36	$19.0 \pm 8.6 \cdot 10^{-6}$
2	1.800	2.840	1.075	50	18.3 ± 8.7
3	1.800	2.580	.999	40	14.2 ± 8.4
4	1.800	2.450	.927	43	21.8 ± 8.9
5	1.800	3.050	1.107	45	7.05 ± 9.2
6	1.800	3.305	1.195	51	6.3 ± 9.4
7	1.800	3.230	1.120	41	5.0 ± 8.6
8	1.510	1.626	.522	17	13.8 ± 10.7

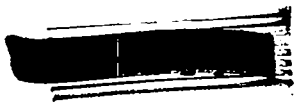

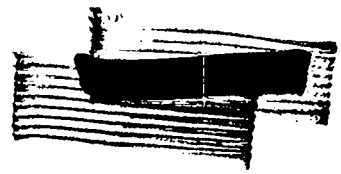

APPENDIX IV

Series #3

Run No.	Δt Sec.	N_f Counts	N_p Counts	C Coincidences	$\frac{Cr}{N_p}$ Corr.
1	$1.800 \cdot 10^3$	$3.235 \cdot 10^4$	$.752 \cdot 10^6$	41	$20.4 \pm 11.10 \cdot 10^{-6}$
2	1.800	3.180	.985	60	27.7 ± 10.15
3	1.800	2.981	1.020	66	33.5 ± 10.00
4	1.800	3.010	1.075	53	17.8 ± 9.02
5	1.800	3.300	.831	37	9.82 ± 10.05
6	1.800	3.001	.697	38	22.9 ± 11.40
7	1.764	2.685	1.025	54	24.2 ± 9.22
8	1.765	2.440	.882	37	15.83 ± 9.07
9	1.800	2.680	.721	37	23.20 ± 10.72
10	1.800	3.145	.977	37	4.75 ± 8.88
11	1.800	2.590	.990	39	13.50 ± 9.32
12	1.800	2.525	.967	39	15.40 ± 9.82
13	1.800	2.580	.955	38	16.20 ± 9.44
14	1.800	1.505	.419	15	20.2 ± 11.2
15	1.800	1.770	.512	17	14.55 ± 10.3
16	1.800	1.835	.550	18	15.52 ± 9.92
17	1.800	1.745	.470	18	20.05 ± 11.15
18	1.788	1.617	.442	19	26.10 ± 11.86
19	1.800	3.970	1.213	79	23.30 ± 10.24
20	1.800	3.520	1.184	60	14.08 ± 8.97

[redacted]